Published in final edited form as:
J Comp Neurol. 2008 November 1; 511(1): 47–64. doi:10.1002/cne.21827.

Ultrastructural Analysis of the Cristae Ampullares in the Squirrel Monkey (*Saimiri sciureus*)*

Anna Lysakowski[1] and **Jay M. Goldberg**[2]

[1] Department of Anatomy and Cell Biology, University of Illinois at Chicago, 808 S. Wood St., M/C 512, Chicago, IL 60612, USA

[2] Department of Neurobiology, Pharmacology and Physiology, University of Chicago, 947 E. 58th St., MC 0926, Chicago, IL 60637, USA

Abstract

Type I hair cells outnumber type II hair cells (HCs) in squirrel monkey (*Saimiri sciureus*) cristae by a nearly 3:1 ratio. Associated with this type I HC preponderance, calyx fibers make up a much larger fraction of the afferent innervation than in rodents (Fernández et al., 1995). To study how this affected synaptic architecture, we used disector methods to estimate various features associated with type I and type II HCs in central (CZ) and peripheral (PZ) zones of monkey cristae. Each type I HC makes, on average, 5–10 ribbon synapses with the inner face of a calyx ending. Inner-face synapses outnumber those on calyx outer faces by a 40:1 ratio. Expressed per afferent, there are, on average, 15 inner-face ribbon synapses, 0.38 outer-face ribbons and 2.6 efferent boutons on calyx-bearing endings. Calyceal invaginations per type I HC range from 19 in CZ to 3 in PZ. For type II HCs, there are many more ribbons and afferent boutons in PZ than in CZ, whereas efferent innervation is relatively uniform throughout the neuroepithelium. Despite outer-face ribbons being more numerous in chinchilla than in squirrel monkey, afferent discharge properties are similar (Lysakowski et al., 1995), reinforcing the importance of inner-face ribbons in synaptic transmission. Comparisons across mammalian species suggest the prevalence of type I HCs is a primate characteristic, rather than an arboreal lifestyle adaptation. Unlike cristae, type II HCs predominate in monkey maculae. Differences in hair-cell counts may reflect the stimulus magnitudes handled by semicircular canals and otolith organs.

Keywords

vestibular; hair cells; ribbon synapses; efferent synapses; semicircular canals; otolith organs; maculae

---

There are two types of hair cells in the vestibular organs of amniotes, including reptiles, birds and mammals (Wersäll and Bagger-Sjöbäck, 1974; Lysakowski, 1996). Type I hair cells contact calyx endings; type II hair cells synapse on bouton endings. Type II hair cells, which are also present in fish (Boyle et al., 1991; Lysakowski, 1996) and amphibia (Honrubia et al., 1989; Lysakowski, 1996), are found throughout the vestibular neuroepithelia in most amniotes. In contrast, type I hair cells have a restricted distribution in

*This study was supported by NIH, the National Institute for Deafness and Communication Disorders R01 DC-02521 (AL) and R01 DC-02058 (JMG).

Author for Correspondence: Dr. Anna Lysakowski, Department of Anatomy and Cell Biology, University of Illinois at Chicago, 808 S. Wood St., CME 578, M/C 512, Chicago, IL 60612, USA, Telephone: (312) 996-5990, FAX: (312) 413-0354, e-mail: alysakow@uic.edu.
Associate Editor: Dr. Thomas E. Finger

reptiles (Jørgensen, 1974; Schessel et al., 1991; Brichta and Peterson, 1994; Xue and Peterson, 2006) and birds (Jørgensen and Andersen, 1973; Si et al., 2003; Zakir et al., 2003; Haque et al., 2006), being confined to a central zone in the cristae and to the striola in otolith organs. The saccular macula of birds is an exception to this rule as type I hair cells have a broad distribution throughout much of the neuroepithelim (Jørgensen and Andersen, 1973; Zakir et al., 2003).

That both kinds of hair cells are important in the mammalian vestibular system is suggested by the fact that they occur in almost equal numbers throughout the cristae (Lindeman, 1969; Fernández et al., 1995; Desai et al., 2005a) and otolith organs (Lindeman, 1969; Desai et al., 2005b) of several rodent species. A somewhat different result is found in the squirrel monkey cristae, where type I hair cells considerably outnumber type II hair cells (Fernández et al., 1995). The type I: type II ratio averages 3 : 1 throughout the monkey cristae and varies from 5 : 1 in the central zone (CZ) to < 2 : 1 in the peripheral zone (PZ). A similar preponderance is seen in an Old World monkey (*Macaca mulatta)* (Lysakowski, 1996). It is unclear what is the ratio of the two hair-cell types in monkey otolith organs.

Because of differences in the type I : type II ratio, a comparison between rodents and monkeys may shed light on the distinctive contributions of the two kinds of hair cells. The first thing to note in this regard is that there are similarities in the structural and functional organization of the cristae in mammals. The neuroepithelium can be divided into central and peripheral zones based on their cytoarchitecture and afferent innervation patterns (Fernández et al., 1988, 1995; Leonard and Kevetter, 2002; Desai et al., 2005a). Of the three kinds of afferents, calyx fibers innervate type I hair cells in the CZ and bouton afferents supply type II hair cells in the PZ. Dimorphic fibers, which provide a mixed innervation to type I and type II hair cells, are found throughout the neuroepithelium and their preponderance in a region between the CZ and PZ provides the basis for recognizing an intermediate zone (IZ). This is not to say that the afferent innervation is identical across species. Reflecting the higher proportion of type I hair cells, calyx fibers are more common in the squirrel monkey than in the chinchilla, while dimorphic and bouton fibers are less common (Fernández et al., 1995). Finally, afferent discharge properties are similar in the chinchilla (Baird et al., 1988; Hullar and Minor, 1999; Hullar et al., 2005) and in a variety of monkey species (Lysakowski et al., 1995; Haque et al., 2004; Ramachandran and Lisberger, 2006; Sadeghi et al., 2007).

The cristae have been studied in various rodents. Of these, we have the most information in the chinchilla (Baird et al., 1988; Fernández et al., 1988, 1995; Lysakowski and Goldberg, 1997; Hullar and Minor, 1999; Desai et al., 2005a; Hullar et al., 2005). With one exception, similar information is available for the squirrel monkey (Fernández and Goldberg, 1971; Goldberg and Fernández, 1971a,b; Fernández et al., 1995; Lysakowski et al., 1995). The exception concerns the ultrastructural organization of the cristae, which has been studied in the chinchilla (Lysakowski and Goldberg, 1997), but not in the squirrel monkey. This was one reason for the present study. Another was to consider the physiological implications of structural differences between the two species, especially in light of recent studies of synaptic transmission between type I hair cells and calyx endings (Rennie and Streeter, 2006; Holt et al., 2007).

Concerning physiological implications, a question of particular interest is the source of synaptic activity recorded from calyx endings. While calyx endings receive most of their synaptic input on their inner faces from type I hair cells, they also get inputs from type II hair cells by way of ribbon synapses on their outer faces (Engström, 1970; Lysakowski and Goldberg, 1997; Matsubara et al., 1999). In the chinchilla, inner-face synapses outnumber outer-face synapses by a 5 : 1 ratio in the central zone and by an even larger ratio elsewhere in the neuroepithelium (Lysakowski and Goldberg, 1997). The preponderance of inner-face

synapses suggests that they are particularly important in synaptic transmission. But because of the presence of a distinctive M-like ionic current that lowers the input impedance of the type I hair cell (Correia and Lang, 1990; Rüsch and Eatock, 1996; Hurley et al., 2006), it is conceivable that transduction currents cannot depolarize type I hair cells sufficiently to activate the Ca^{2+} currents thought to be needed to trigger neurotransmitter release (Goldberg and Brichta, 2002; Bao et al., 2003; Hurley et al., 2006; Holt et al., 2007). This raises the possibility that outer-face synapses may be more important than their relative numbers suggest. That type I hair cells can give rise to quantal neurotransmitter release has been demonstrated in recordings from solitary calyx endings in contact with individual type I hair cells (Rennie and Streeter, 2006). However, the rate of quantal activity in this isolated preparation is considerably lower than that seen in the intact turtle posterior crista (Holt et al., 2007). The disparity in rates might be explained by the presence of outer-face synapses in the intact preparation and their absence in the solitary ending. Another test of the relative importance of outer-face synapses is provided by the squirrel monkey cristae. Given the small numbers of type II hair cells in the monkey CZ, outer-face synapses might be rare or non-existent in this zone where calyx fibers reside. Such a finding, if true, coupled with the similarity in the discharge properties of calyx fibers in the chinchilla (Baird et al., 1988; Hullar and Minor, 1999; Hullar et al., 2005) and the squirrel monkey (Lysakowski et al., 1995), would emphasize the importance of inner-face synapses from type I hair cells.

In this paper, we used stereological methods to estimate the numbers of various synaptic and other features found in association with type I and type II hair cells in the squirrel monkey cristae. Structures of interest were ribbon synapses, including those made by type I hair cells with calyx inner faces and those made by type II hair cells with afferent boutons and calyx outer faces, afferent boutons, calyceal invaginations, and efferent boutons (Fig. 1), as well as the subsurface cisterns associated with the latter two structures. In considering the functional consequences of our results, it became of interest to determine the relative proportions of type I and type II hair cells in monkey otolith organs and this was done in light-microscopic material.

MATERIALS AND METHODS

Ultrastructural studies of the squirrel monkey crista

Tissue preparation—Three adult male squirrel monkeys (*Saimiri sciureus*), weighing 600–800 g, were anesthetized with sodium pentobarbital (40 mg/kg) and perfused transcardially with 100–200 ml of a warm 0.1M sodium cacodylate-0.9% NaCl buffer (pH 7.4), followed by 1000 ml of a warm trialdehyde fixative, consisting of 3% glutaraldehyde, 2% paraformaldehyde, 1% acrolein, and 5% sucrose in 0.08 M cacodylate buffer (DeGroot et al., 1987). During perfusions, animals were artificially respired to minimize anoxia. Individual endorgans were dissected, postfixed for 1 hour in either 1% OsO_4 or 1% OsO_4/1.5% $K_4Fe(CN)_6 \cdot 3H_2O$ in 0.1 M cacodylate buffer, stained *en bloc* with uranyl acetate in 70% ethanol, dehydrated in graded ethanol and propylene oxide solutions, and embedded in Araldite. Experiments were approved by the University of Chicago Institutional Animal Care and Use Committee.

Material came from three cristae (one superior, another posterior and the third horizontal), each from a different animal. Cristae were sectioned transversely. Serial sections, 5 μm thick, were cut with glass knives through the whole endorgan and mounted on glass slides. It was important that each section pass through all three zones of the crista (see below for a delineation of zones). This necessitated that the sections chosen for ultrastructural examination not be near the longitudinal edges abutting the planum semilunatum. Sections were remounted on prepared Araldite blocks, serially sectioned with a diamond knife,

collected on 2-mm formvar-coated slot grids, and stained with uranyl acetate and lead citrate.

Data acquisition—Thirty consecutive ultrathin (75–nm) sections constituted a sample. For each of the two vertical cristae, three samples were examined in the electron microscope (EM). Each sample was taken from a separate semithin section. Only one 30-section sample from the horizontal crista was studied. Figure 2 shows the locations of the samples. One set of samples was from the center of the crista (Fig. 2 A); the other two were more eccentrically placed (Fig. 2 B, C). Low-power (×2,000) micrographs were taken of every fifth ultrathin section (≈0.3 μm apart) and a photomontage (×5,000 final magnification) was made of the entire neuroepithelium contained in the section. All hair-cell nuclei in each sample were identified. Ribbon synapses were counted by direct examination of serial sections. Afferent boutons, calyceal invaginations, and efferent boutons were identified in the montages and confirmed ultrastructurally. Electron micrographs for publication were taken on film in a JEOL 1220 transmission electron microscope and printed on photographic paper. The photos and/or negatives were digitally scanned and labeling was done in Adobe Photoshop CS2. Light micrographs were taken on a Leica DM6000B research microscope using Leica Application Suite software and labeling was done in Adobe Photoshop CS2.

Zones of the crista—For quantitative analysis, the neuroepithelium was divided into central, intermediate and peripheral zones of equal areas (CZ, IZ, and PZ, respectively) (Fernández et al., 1995). As in previous studies, the boundaries between the three areas were taken as $\pm 1/\sqrt{3}$ and $\pm\sqrt{2}/\sqrt{3}$ of the distances measured along the top on the neuroepithelium from its midpoint to its edges. Note that, in the transverse sections used in this study, the CZ, IZ and PZ make up 58%, 24% and 18% of the total linear distance, respectively (Fig. 3 A).

Number of hair cells and hair-cell ratios—The equivalent numbers of type I and type II hair cells were estimated in each sample by counting the corresponding nuclei with the disector technique (Gundersen, 1986), as was previously done (Fernández et al., 1995; Lysakowski and Goldberg, 1997; Desai et al., 2005a,b). The two kinds of hair cells were easily distinguished from supporting cells and from each other. Of the three populations, supporting-cell nuclei are most irregularly shaped, have much denser heterochromatin, and are located closest to the basal lamina (Fig. 3B). Type I hair cells, unlike type II hair cells, are surrounded by calyx axoplasm. Every type I and type II nucleus present in the first ("reference") section of the 30-section sample, but not in the last ("lookup") section, was counted. As nuclear size is larger than the sample thickness of 2.25 μm, no nucleus fell entirely within the sample. For this reason, reversing the order of the reference and lookup sections provided a second, independent count of nuclei. The two counts were averaged to give Q^{-}, an estimate of the equivalent number of hair cells contained in the sample.

Number of synaptic elements per hair cell—Double counting of synaptic structures was avoided by not counting any element found in the lookup section. The number of elements per hair cell was expressed as a ratio with the number of hair cells (Q^{-}) in each disector sample. Ratios were obtained for each synaptic structure listed in Tables 2 and 3, and were separately compiled for type I and type II hair cells in the various zones of the crista. We were also interested in the number of synaptic elements made on calyx endings of each calyx-bearing (calyx or dimorphic) fiber, reflecting the presence of simple and complex endings innervating, respectively, one or more type I hair cells, as well as the presence of multiple endings. To obtain these estimates, we multiplied the estimates per hair cell by a factor of 1.83, the average number of calyx endings per afferent previously determined (Fernández et al., 1995). The factors were similar for calyx (1.86 ± 0.072) and dimorphic units (1.80 ± 0.054).

Hair-cell counts in otolith organs

It became of interest to compare hair-cell ratios in the cristae and otolith organs. This was done by light microscopy (LM). Four squirrel monkeys were anesthetized and perfused transcardially as described above. Individual organs were dissected and embedded in Araldite. Four utricular and two saccular maculae were serially sectioned with glass knives in transverse planes (Fig. 2D, E). For each 50 μm of tissue, we collected 10 consecutive 2-μm sections, followed by two 5-μm sections and two 10-μm sections, and mounted them on glass slides. Slides were placed on a hot plate, and sections were stained by covering each of them with a drop of a warm mixture of 1% azure II, 2% methylene blue, and 2% sodium borate (Richardson et al., 1960).

Hair-cell nuclei were counted by disector techniques from two consecutive 2-μm sections in each 50-μm set. Separate counts were obtained from the striola and from the extrastriola to either side of the striola. We used hair-bundle morphological polarization to locate the striola. Previous workers had concluded that the midpoint of the striola corresponded to the place where hair bundles reversed polarity, the line of polarity reversal (LPR) (Lindeman 1969; Rosenhall 1972; Lim 1984). A recent study (Li et al., 2007) showed that in the mouse utricular macula the LPR lies immediately lateral to the striola. Because the situation in the monkey is unclear, we made two utricular counts, one with the LPR lying in the middle of the striola and the other with the reversal line defining the lateral border of the striola. For the saccular macula, we took the LPR as the center line of the striola. In all cases, the striolae were assumed to be 100 μm wide.

Statistical procedures

Unless otherwise stated, statistical values are expressed as means ± SEM. Mean ratios between the incidence of two structures (*X* and *Y*), e.g., the number of synapses *(Y)* and the number of hair cells *(X)* were calculated as $\Sigma Y_i/\Sigma X_i$, where each summation was over all seven samples (Fig. 2A–C). SEMs for ratios were based on a formula in Bulmer (1979). Unless otherwise stated, two-sided Wilcoxon tests were used to assess the statistical significance of differences.

RESULTS

As in a previous study (Lysakowski and Goldberg, 1997), we combined EM data from the superior, posterior and horizontal cristae as we could find no difference between them or between the more centrally placed (Fig. 2A) or more eccentrically placed samples (Fig. 2B, C). LM hair-cell counts were done separately for the utricular and saccular maculae.

Stereological counts in the cristae

Numbers of type I and type II hair cells—A transverse, semithin section through the middle of a superior crista illustrates the relative numbers of type I and type II hair cells (Fig. 3A). Only five of the 31 hair-cell nuclei found in the section belong to type II hair cells.

Table 1 includes hair-cell counts from the present EM study and from a previous LM study in the monkey (Fernández et al, 1995), as well as previously published LM and EM counts for the chinchilla (Fernández et al, 1995;Lysakowski and Goldberg, 1997). The relative paucity of type II hair cells seen in Figure 3A is confirmed by disector counts based on seven ultrathin samples. As in the previously published LM samples for the monkey, the ratio is highest in the CZ and lowest in the PZ. Nevertheless, the central-to-peripheral gradient in the type I : type II ratio is smaller in the present sample than in the previous LM material (3.2 : 2.0 versus 5.2 : 1.5). Averaged over all zones, the type I : type II ratio of 2.8

is virtually identical in the EM and LM samples. The coincidence may be misleading. The LM material was based on evenly spaced semithin sections taken throughout the crista and shows that the predominance of type I hair cells is consistent throughout the end organ. In contrast, the EM samples, as a result of passing through all three zones, overemphasize the CZ (see MATERIALS AND METHODS, Zones of the crista). When the percentages of the three zones in our EM sections are taken into account, the type I : type II ratio, based on the LM material, should be 4.3 ± 0.6, somewhat higher than the ratio actually observed, 2.8 ± 1.0; the difference was not statistically significant (two-sided *t* test, $p > 0.2$). The present EM sample confirms the preponderance of type I hair cells in the monkey as compared to the chinchilla.

Numbers of synaptic elements—Disector counts, summarized in Table 2 for type I hair cells and in Table 3 for type II hair cells, provide an overview of our ultrastructural observations. Included in the tables are previously published counts from the chinchilla (Lysakowski and Goldberg, 1997). There are typically 5–10 ribbon synapses in each monkey type I hair cell, fewer than seen in the chinchilla. Calyceal invaginations in monkey type I hair cells, which again are less numerous than in the chinchilla, show a central-to-peripheral gradient in both species. A statistically significant gradient is not seen in the number of inner-face ribbons or of efferent boutons contacting calyx endings in the monkey. Synapses between type II hair cells and calyx outer faces are common in the CZ of the chinchilla and infrequent in the PZ. Given the paucity of type II hair cells in the monkey's CZ, it is not surprising that outer-face calyx synapses are infrequently seen there. Nor are such synapses common elsewhere in the crista. To calculate the number of synapses on calyx endings per afferent, we multiplied entries in the last row of Table 2 by 1.83, an estimate of the number of type I hair cells innervating each calyx or dimorphic afferent (see MATERIALS AND METHODS, Number of synaptic elements per hair cell). On average, the calyx endings of each calyx-bearing afferent were contacted by 15.2 ± 1.6 inner-face ribbon synapses and by 2.6 ± 0.5 efferent boutons.

The overall number of afferent boutons on type II hair cells, as well as the number of afferent boutons and of ribbon synapses made by each type II hair cell are similar in the two species, as is the presence of a regional variation in the frequencies of afferent boutons (Table 3). On the other hand, a regional variation in the number of ribbon synapses on afferent boutons was only seen in the monkey. The efferent innervation of type II hair cells (Table 3) is similar in the squirrel monkey and chinchilla and is relatively uniform throughout the crista of either species.

Synaptic relations in the cristae

Having summarized our stereological findings, we illustrate synaptic relations with individual examples of type I and type II hair cells in the CZ and PZ.

Type I hair cells, central zone—Calyx endings can be simple or complex. Simple endings enclose single hair cells, whereas complex endings innervate two or more hair cells. Complex endings are especially common in the CZ. An example is seen in Figure 4, where two type I hair cells (16L and 16R) are contained within a complex ending. Also included in the figure are the nuclei of five supporting cells (SC). In the 30-section sample, cells 16L and 16R had four and five ribbon synapses, respectively (Fig. 4, *arrows* and *inset*); each hair cell had eight invaginations. As there were no type II hair cells in the field, no outer-face ribbons were found. Nor did any efferent bouton contact the calyx ending. It should be emphasized that hair cells were only examined in 30-section disectors. Based on the estimates of cell size, less than one-half of any hair cell might be contained in the sample. That the particular hair cells in Figure 4 were incompletely sectioned was verified by

inspection of the sample's first and last sections. At the beginning of the sample, both hair cells and their nuclei were well developed. By the sample's end, one of the cells (16L) had greatly diminished in size and its nucleus was no longer present. The other cell and its nucleus were still conspicuous.

One consequence of incomplete sampling is that there is an underestimate of the incidence of complex calyces. We know this because in a previous study of dye-filled, completely reconstructed calyces, 36% of these endings were complex (Fernández et al., 1995), as compared to 14% in the present study. As in the earlier study, we find that complex endings make up a larger fraction of calyces in the CZ than in the PZ, where only 4.3% of the endings were complex. Once again, the percentage of complex endings in the PZ is underestimated from the 17% observed in dye-filled material. The complex ending in Figure 4 was flanked by supporting cells. Even the calyx ending of cell 17, although it comes close to the complex ending, is separated from the latter by a supporting-cell sliver.

To gain some appreciation as to the reasons for the paucity of outer-face synapses, we counted the number of appositions between calyx endings and type II hair cells, as well as the number of outer-face synapses. Results are summarized in Table 4. Less than one-fourth of the appositions in the CZ and IZ and none in the PZ are associated with an outer-face ribbon. The discrepancy between the frequencies of appositions and outer-face ribbons suggests that the small number of such synapses and their absence from the PZ cannot be explained merely by a lack of type II hair cells.

Type II hair cells, central zone—Type II cell 34 was contacted by four afferent boutons, of which three are present in Figure 5 (Fig. 5). None of the boutons was completely contained in the sample. There was a ribbon synapse on bouton 3 *(arrow)*. As was typical of type II hair cells, synaptic ribbons were located below the nucleus. The type II hair cell was separated from the two neighboring type I hair cells (33 and 35) by supporting-cell processes. No efferent synapses were seen.

Peripheral zone—Figure 6 illustrates the synaptic features of the PZ. A type I hair cell (60) is flanked by two type II hair cells (59 and 61). Consistent with the relatively low average counts for peripheral type I hair cells in Table 2, cell 60 had one ribbon and no invaginations. Its calyx ending was contacted by one efferent bouton *(E3)*. As can be seen in Table 3, PZ type II hair cells are contacted by many afferent boutons, with which they make ribbon synapses. These trends are illustrated by the two type II hair cells in Figure 6. Cell 59 had nine afferent and three efferent boutons, plus three ribbon synapses (Fig. 6). The numbers for the other type II hair cell (61) were 10 afferent boutons, three efferent boutons and 11 ribbon synapses. One of the efferent boutons on cell 59 (E2) also made synapses with both the calyx ending of cell 60 and with cell 61. Cell 59 had thin slivers of supporting cells separating it from type I cells 58 and 60. In contrast, cell 61 made three appositions with calyces, two short ones with the calyx of cell 60 and one long one with the ending of cell 62L. Despite the appositions, no outer-face ribbons were made by this or any other peripheral type II hair cell in our samples.

Morphology of ribbon synapses—Synaptic ribbons in type I hair cells, regardless of zone, were typically small (≈100 nm) and spherical (Fig. 4, *inset*; Fig. 7 A, B). This may be contrasted with the observations of Engström and colleagues (Engström, 1970;Engström et al., 1972), who found that synaptic ribbons in type I hair cells of the squirrel monkey macular organs could be quite elongated.

Ribbons between central type II hair cells and bouton endings were more variable. They could be round (Fig. 7C, D, H, J–L) or, less frequently, elongated (Fig. 7G, I) and ranged in

size from 100 nm to 300 nm. Both solid (Fig. 7D–F, H–J) and hollow synaptic ribbons (Fig. 7K,L) were seen with the former being more common. Rarely, synapses had multiple ribbons sharing vesicles (Fig. 7E, F). It is difficult to generalize about outer-face synapses because there were so few of them (15 outer-face vs. 1231 total ribbons). Three examples are seen in Figure 7. One had multiple ribbons (Fig. 7E, F). The other two had single synaptic ribbons, one of which was small, elongated and slightly hollow (Fig. 7G), whereas the other was a little larger and solid (Fig. 7H).

Ribbons in PZ type II hair cells were small, round and solid (Fig. 7J) or, less frequently, were hollow (Fig. 7K, L) and could vary in size.

Efferent synapses, invaginations and subsurface cisterns—As has been described previously (Engström, 1958; Smith and Rasmussen, 1967), efferent terminals are recognized by being highly vesiculated. Those efferents contacting hair cells are marked by a subsynaptic cistern (Fig. 8 A, arrows); efferent synapses on afferent processes have presynaptic and postsynaptic thickenings (Fig. 8B). Efferent synapses are found at the base of calyces, on other afferent processes near their terminations on type II hair cells, and on the latter hair cells at infranuclear or, less frequently, at nuclear and supranuclear levels. The same efferent process can contact afferent processes, including calyces, as well as type II hair cells. Invaginations of calyx endings into the type I hair cell are associated with a reduction in the intercellular cleft (Spoendlin, 1966; Gulley and Bagger-Sjöback, 1979); a new finding in the present paper is that the endoplasmic reticulum (ER) is in close association in about a quarter (48/186) of the invaginations (Fig. 8C). Another novel observation is that the ER, when it makes an subsurface cistern in type I hair cells, is commonly associated with a narrowing of the intercellular space, which sometimes has an undulating appearance (Fig. 8D). The narrowing of the synaptic cleft is similar to that seen in invaginations (from 20 nm normally to 7 nm). Both the association of the ER with calyceal invaginations and the narrowing of the synaptic cleft adjacent to the subsurface cisterns have also been observed in type I hair cells of the rat and chinchilla (Lysakowski, unpublished observations).

Hair-cell counts in monkey otolith organs

Type I hair cells predominate in the monkey crista. To provide a context for this finding, we used LM material to make hair-cell counts in monkey otolith organs. Methods were similar to those previously published (Fernández et al., 1995; Desai et al., 2005b). We had suspected that the otolith organs would resemble monkey cristae in having a preponderance of type I hair cells or else be similar to rodent otolith organs in having similar numbers of type I and type II hair cells. To investigate these possibilities, hair-cell counts were done in four utricular and two saccular maculae (Fig. 9 and Table 5).

The total number of hair cells in the utricular macula outnumbered that in the saccular macula (Table 5), as had previously been found in the squirrel monkey (Igarashi et al., 1975), in man (Rosenhall, 1972) and in several, but not all rodents (Lindeman, 1969;Watanuki and Meyer zum Gottesberge, 1971;Desai et al., 2005b). Counts in both squirrel-monkey organs were larger than those reported by Igarashi et al. (1975), which likely reflects differences in histological and in counting procedures. Our estimates for both otolith organs were considerably larger than those obtained with similar methods in smaller rodents (mouse, rat, gerbil, and guinea pig), but only slightly larger than those in larger rodents (chinchilla, tree squirrel) (Desai et al., 2005b), and considerably smaller than those in humans (Rosenhall, 1972). Densities in hair cells per 100 μm^2 for the two organs (utricle = 1.84 ± 0.09, saccule = 1.72 ± 0.04) were statistically indistinguishable ($p > 0.03$) and were somewhat higher than found in rodents (Desai et al., 2005a). Combining data for the two

organs, striolar densities were ≈10% lower than extrastriolar densities; the last result was barely insignificant ($p < 0.06$).

Contrary to expectations about the complement of the two hair-cell types, type II hair cells outnumbered type I hair cells in both the utricular and saccular maculae (Fig. 9). Disector counts gave a type I : type II ratio of 0.59 ± 0.06 for the utricular macula and 0.53 ± 0.06 for the saccular macula. In short, type II outnumbered type I hair cells by a 1.75 : 1 ratio. Similar ratios were seen in the striola and in extrastriolar regions of either organ. The ratios for the utricular macula did not depend on the precise boundary of the striola. The preponderance of type II hair cells is unlike that reported in any rodent species (Lindeman, 1969;Watanuki and Meyer zum Gottesberge, 1971;Desai et al., 2005b).

DISCUSSION

This is the first systematic ultrastructural examination of the synaptic innervation in the monkey crista. It was prompted by a previous paper (Fernández et al., 1995) showing that the complements of type I and type II hair cells differed in the monkey and the chinchilla. In this section, we: 1) compare the ultrastructural organization of the cristae in the two species; 2) discuss the implications of the structural differences for physiology, particularly synaptic transmission in type I hair cells; 3) consider comparative trends in the morphology of vestibular organs; and 4) use the difference between the cristae and otolith organs in their type I : type II ratios to speculate about the function of calyx fibers.

Comparing the ultrastructural organization in the squirrel monkey and chinchilla

There are several differences in synaptic features between the two species. The chinchilla data are from Lysakowski and Goldberg (1997). We first consider type I hair cells (Table 2). Fewer inner-face ribbons and calyceal invaginations are found in the monkey. While there is a regional variation in invaginations in both species, a similar variation in ribbon synapses was only seen in the chinchilla. Efferent boutons terminating on calyx endings were less common in the monkey. Turning to type II hair cells (Table 3), the average numbers of ribbon synapses, afferent boutons and efferent boutons per hair cell are similar in the two species. Two differences involving type II hair cells can be mentioned: 1) there is a regional variation in synaptic ribbons and afferent boutons in the monkey, but not in the chinchilla; and 2) the similar numbers of ribbons and afferent boutons in the monkey CZ imply that most bouton endings make a single synapse with type II hair cells. In contrast, we previously observed relatively large afferent boutons in the chinchilla CZ that were contacted by multiple synapses.

None of the aforementioned differences are related in any obvious way with the difference in type I : type II ratios between the two species. The one difference that may reflect the complement of the two hair cell types is the number of outer face ribbons. This type of synapse, first described by Engström (1970), was found to be relatively common in the central zone of the rodent crista (Goldberg et al., 1990c; Lysakowski and Goldberg, 1997; Matsubara et al., 1999). In part reflecting the paucity of type II hair cells, there are very few such synapses in the monkey CZ. While there are, on average, 2.9 outer-face ribbons per type I hair cell in the chinchilla CZ, the comparable figure for the squirrel monkey is 0.2. Taking into account the typical number of type I hair cells contacted by calyx and dimorphic fibers, >60% of the afferents in the monkey CZ do not get even a single outer-face synapse, whereas each afferent similarly located in the chinchilla gets an average of 4.7 such synapses. Another perspective is provided by the ratio of inner-face to outer-face ribbons in the central zone. The ratio is 7.6 : 1 in the chinchilla and 42 : 1 in the monkey. While these numbers parallel the ratio of type I to type II hair cells in the two species, other factors must come into play. In particular, there are almost no outer-face ribbons in the PZ of either

species even though there are plenty of type II hair cells (Table 1) and appositions (Table 4) in this part of the crista.

Implications for synaptic transmission

Our ultrastructural findings bear on the mechanisms of synaptic transmission. In particular, what are the relative contributions of inner-face and outer-face ribbons to the synaptic input of calyx endings? The large numbers of inner-face ribbons (Lysakowski and Goldberg, 1997; Holt et al., 2007; the present study) and of AMPA receptors on the calyx inner face (Matsubara et al., 1999) should dispel doubts about this matter. Yet, the presence of an M-like current ($I_{K,L}$) lowers the input impedance and hyperpolarizes the type I hair cell, so much so that the possibility of quantal transmission to the inner face has been questioned (Goldberg, 1996; Bao et al., 2003; Hurley et al., 2006; Holt et al., 2007). In this respect, the electrophysiology of type I hair cells is similar in turtles (Brichta et al., 2002; Goldberg and Brichta, 2002), pigeons (Correia and Lang, 1990; Rennie and Correia, 1994), and mammals (Rennie and Correia, 1994; Rüsch and Eatock, 1996). Quantal activity has been recorded in an isolated preparation consisting of single calyx endings innervated by individual type I hair cells in the gerbil (Rennie and Streeter, 2006). While outer-face synapses are not present in the isolated calyx preparation, quantal rates were much lower (20/s) than in the intact turtle posterior crista (1000/s) (Holt et al., 2007), the only other preparation in which synaptic activity has been recorded from calyx afferents. In fact, quantal rates in the isolated calyx preparation are much too low to sustain the high background discharge rates seen in mammalian calyx afferents (40–100 spikes/s) (Lysakowski and Goldberg, 2004). The difference in quantal rates between the isolated and intact preparations could be explained by the trauma involved in isolating the calyx ending and hair cell. Another possibility is that outer-face synapses, which are plentiful in the intact turtle preparation, are responsible.

Because of this last possibility, it becomes of interest to evaluate the physiology of vestibular-nerve fibers in the presence and near-absence of outer-face synapses. This can be accomplished by comparing discharge properties in the chinchilla (Baird et al., 1988; Hullar et al., 2005) and the squirrel monkey (Lysakowski et al., 1995). The simplest comparison is between calyx units in the two species. These units can be distinguished by their relatively low rotational gains at midband frequencies and their irregular discharge. Remarkably, the gains of calyx units are almost identical in the two species despite the almost complete absence of outer-face synapses in the squirrel monkey. The results imply that inner-face synapses are a major source of synaptic activity in monkey calyx afferents. While outer-face synapses may make a more substantial contribution in the chinchilla calyx units, there is little reason to suppose that they are more important than their relative numbers suggest.

A related issue is whether type I hair cells are capable of quantal neurotransmitter release at physiological rates such as those occurring at other hair-cell synapses (Furukawa et al., 1972; Glowatzki and Fuchs, 2002; Keen and Hudspeth, 2006) including those involving type II vestibular hair cells (Rossi et al., 1994; Holt et al., 2006). Here, discharge regularity is relevant. As is the case for calyx afferents in the chinchilla (Baird et al., 1988; Hullar et al., 2005), those in the squirrel monkey (Lysakowski et al., 1995) and in macaque monkeys (Haque et al., 2004; Ramachandran and Lisberger, 2006; Sadeghi et al., 2007) have an irregular discharge. The variability of interspike-intervals in an irregular discharge requires synaptic noise. There are two potential sources of such noise: 1) channel noise resulting from the stochastic opening and closing of channels; and 2) quantal noise, the shot-noise produced by individual mEPSPs. Direct measurements indicate that of the two sources of noise only quantal noise is large enough to produce an irregular discharge with channel noise contributing only about 1% of the total synaptic noise (Holt et al., 2006; also see Smith and Goldberg, 1986). It follows that the calyx ending must be a recipient of quantal activity and, in the virtual absence of outer-face synapses in the squirrel monkey, this must

arise from type I hair cells. The large numbers of ribbon synapses in type I hair cells of the chinchilla (Lysakowski and Goldberg, 1997) and turtle (Holt et al., 2007) suggest that quantal transmission is a general characteristic of such hair cells.

If, as we suggest, quantal transmission occurs between type I hair cells and calyx ending, then how are the effects of $I_{K,L}$ circumvented? Two mechanisms have been proposed. The first is that K^+ ions, released from the basolateral surface of the hair cell during transduction, depolarize the hair cell sufficiently to result in quantal neurotransmitter release (Goldberg, 1996; Eatock and Lysakowski, 2006). Second, the activation (I–V) curve of $I_{K,L}$ may be sufficiently shifted in a depolarizing direction by nitric oxide or some other agent so that the current no longer impedes quantal release (Behrend et al., 1997; Chen and Eatock, 2000). Regardless of the mechanisms negating the effects of $I_{K,L}$, the combined physiological and ultrastructural results in the squirrel monkey (Lysakowski et al., 1995), together with the presence of quantal activity in the isolated calyx preparation (Rennie and Streeter, 2006), provide strong evidence for quantal release from type I hair cells.

The similarity in discharge properties between the squirrel monkey and chinchilla raises a question, which again can be illustrated by calyx units. We have seen that the mid-frequency gains for the two species are nearly identical. Yet, the number of synapses terminating on calyx endings in the central zone is quite different, being about 2.5× higher in the chinchilla, whether we only consider inner-face synapses or include outer-face synapses (Table 2). This would imply that the number of synapses is a poor predictor of gain. This conclusion is consistent with previous morphophysiological results where we found that the number of calyx and bouton endings could not explain the gains within either calyx or non-calyx groups (Baird et al., 1988;Goldberg et al., 1990b). This was so even when gains were corrected for differences in the sensitivity of the postsynaptic spike encoder. Implicit in the approach is the simplistic assumption that there was a fixed ratio in the synaptic input received by individual calyx and bouton endings. Contrary to this assumption, each stage of hair-cell transduction can be a source of synaptic variability (Eatock and Lysakowski, 2006). To cite specific examples, postsynaptic voltages can be modified by the activation of ion channels in the calyx ending (Holt et al., 2007) and possibly by the phosphorylation status and trafficking of receptors (Malenka and Bear, 2004;Ziff, 2007).

Comparative trends in vestibular organs

Is the predominance of type I hair cells in the squirrel monkey crista a general trend found in primates or a specific adaptation to an arboreal lifestyle? A similar preponderance is found in macaque monkeys (Lysakowski, 1996), which unlike the squirrel monkey, are semi-terrestial (Nowak and Paradiso, 1983). In contrast, a type I : type II ratio near unity is found in the tree squirrel (Desai et al., 2005a). This suggests that the type I predominance is not related to lifestyle. What about humans? Here, results are controversial, with one study finding a type I predominance (Merchant et al., 2000) and another study reporting a ratio near unity (Lopez et al., 2005). Quite to our surprise, type II hair cells outnumbered type I hair cells in both otolith organs of the squirrel monkey. It must be emphasized that this finding is unprecedented in the literature, which is largely concerned with rodents (Lindeman, 1969; Watanuki and Meyer zum Gottesberge, 1971; Desai et al., 2005b). Once again it is instructive to compare the squirrel monkey with the tree squirrel, since both have an arboreal life style. Unlike our findings in the squirrel monkey, type I outnumber type II hair cells in squirrel otolith organs (Desai et al., 2005b). In fact, the squirrel utricular macula has a relatively high type I : type II ratio compared to other rodents.

It would be of interest to extend this line of inquiry to a broader range of species. This is becoming increasingly possible as the morphology of vestibular organs is being examined in more species and is being correlated with afferent physiology (reviewed by Lysakowski and

Goldberg, 2004). We confine our attention to the cristae because a relatively complete comparative survey of otolith organs is already available (Zakir et al., 2003). It has been suggested that the cristae have changed from a purely longitudal organization in fish and amphibia to a mixed longitudinal and concentric organization in reptiles and birds and to a purely concentric organization in mammals (Goldberg and Brichta, 1998; Lysakowski and Goldberg, 2004). These changes are correlated with the absence of type I hair cells in fish and amphibia, their restricted distribution in the cristae of reptiles and birds, and their presence throughout the neuroepithelium of mammals. The scheme is reinforced by morphophysiological studies correlating terminal morphology and neuroepithelial location with afferent physiology in fish (Boyle et al., 1991), frogs (Honrubia et al., 1989; Myers and Lewis, 1990), reptiles (Schessel et al., 1991; Brichta and Goldberg, 2000) and mammals (Baird et al., 1988; Lysakowski et al., 1995).

Nevertheless, these comparisons are far from definitive not only because relatively few species have been studied, but also because data are only available for extant animals. Possibly because of these limitations, there is little evidence for specific adaptations to lifestyles. Along these lines, the morphological organization of the cristae is similar in the turtle (Brichta and Peterson, 1994; Igic and Brichta, 1997; Ali et al., 2004) and the pigeon (Ali et al., 2004; Haque et al., 2006) despite the difference in their behavioral repertoires. There is at least one other difference between these species. It has to do with the numbers of type I hair cells enclosed in complex calyces. The number is much smaller in the turtle (Brichta and Peterson, 1994; Igic and Brichta, 1997; Ali et al., 2004) than in the pigeon (Ali et al., 2004; Haque et al., 2006) and even smaller in mammals (Fernández et al., 1995; Desai et al., 2005a).

The more general question of “Why have type I hair cells evolved?” can be considered from different viewpoints: 1) Did they arise as an adaptation to the move from an aquatic (anamniote) to a terrestrial lifestyle (amniote), a transition accompanied by the development of a more flexible neck (discussed in Eatock and Lysakowski, 2006)? 2) The question of lifestyle (arboreal vs. terrestrial), addressed above, is relevant. A study comparing ground-dwelling birds (e.g., ostrich or quail) with flight birds (e.g., pigeons or songbirds) would also be interesting. 3) Regarding the large numbers of type I hair cells that have been reported in complex calyces in a few species of reptiles and birds that was mentioned above, a interesting question is: Do animals that move in three-dimensional space (e.g., turtles in water, or birds in air) have more type I hair cell innervation per afferent? Up to 8 type I hair cells have been observed per turtle calyx fiber (Ali et al., 2004), and up to 16 in pigeon calyx fiber (Haque et al., 2006), compared to as many as 6 per calyx fiber in arboreal tree squirrels (Desai et al., 2005a,b)? Species with large three-dimensional ranges, such as sperm whales (Nowak and Paradiso, 1983), hummingbirds (Altshuler et al., 2004; Tobalske et al., 2007), and frigate birds (Weimerskirch et al., 2003) would also be interesting to study. 4) Finally, response to high frequency displacements has been suggested as another reason for the evolution of type I hair cells (Eatock and Lysakowski, 2006). Examining vestibular endorgans from animals that move in high-velocity bursts (e.g., cheetahs – 70 mph, swifts – 106 mph, peregrine falcons – 200 mph diving speed), compared to animals moving at low-velocity (e.g., three-toed sloths – 6 hpm), may help to clarify this issue. Studying the velocity at which animals move relative to the organization of their vestibular organs and afferents may elucidate the adaptive pressures on hair cells that allow them to accommodate the visual and locomotion challenges produced by the speed of such movements.

Canal versus otolith organs: a possible function of calyx afferents

Previous studies have shown that calyx afferents in the cristae have much lower gains for mid-frequency rotations than do irregular dimorphic afferents. This is so in the chinchilla (Baird et al., 1988; Hullar et al., 2005), the squirrel monkey (Lysakowski et al., 1995), and

macaque monkeys (Haque et al., 2004; Ramachandran and Lisberger, 2006; Sadeghi et al., 2007). In contrast, morphophysiological studies of the utricular macula in the chinchilla indicate that calyx and irregular dimorphic afferents have comparable gains (Goldberg et al., 1990b). The present study provides a second difference between canal and otolith organs. In the squirrel monkey, type I hair cells predominate over type II hair cells in the semicircular canals; the reverse is true in this animal's otolith organs. A different situation occurs in rodents where there are approximately equal numbers of type I and type II hair cells in both the canals (Lindeman, 1969; Fernández et al., 1995; Desai et al., 2005a) and otolith organs (Lindeman, 1969; Desai et al., 2005b). Based on these findings, we speculate that the low gains of calyx afferents in the cristae broaden their dynamic ranges so that they can respond linearly to even quite rapid head movements. Furthermore, the relatively high gains of calyx units in otolith organs may reflect the limited range of linear forces that occur in everyday life.

We start with the rotational stimuli processed by the semicircular canals. Rapid head saccades have been characterized in the squirrel monkey (Armand and Minor, 2001). We can calculate the responses to such head movements using the average velocity and acceleration gains of calyx afferents and linear superposition (Fernández and Goldberg, 1971; Lysakowski et al., 1995). The response of a typical calyx afferent has a peak of 400 spikes/s, approaching the upper limit of excitatory responses in vestibular afferents (Plotnik et al., 1999; Sadeghi et al., 2007). A comparable calculation for irregular dimorphic afferents gives a peak response >1000 spikes/s, well above excitatory saturation. The linear accelerations occurring during everyday activity, which are encoded by otolith organs, are of limited magnitude, <1g for walking and <2 g for running and hopping (Pozzo et al., 1990). Similar stimulus magnitudes occur during other, non-locomotor activities (MacDougall and Moore, 2005). From maximal gains of irregular otolith afferents, whether calyx or dimorphic (Fernández and Goldberg, 1976b; Goldberg et al., 1990a; Angelaki and Dickman, 2000), peak excitatory responses should be on the order of 400 spikes/s, which is within the upper response limits of many otolith afferents (Fernández and Goldberg, 1976a).

These considerations suggest that a distinctive function of calyx afferents in the cristae is the presence of an extended dynamic range allowing the encoding of large-magnitude stimuli. While the hypothesis is attractive, it raises several questions. First, the ability of such fibers to have a large stimulus dynamic range is based on their low rotational gains. It is unclear why a low gain would require the elaborate structures of the type I hair cell and the calyx ending. Second, why should calyx fibers in the semicircular canals have relatively low gains, while those in the utricular macula do not (Baird et al., 1988; Lysakowski et al., 1995; Goldberg et al., 1990b)? An analysis suggested that synaptic transmission involving calyx endings was similar in canal and otolith organs and that other factors led to the high gains of the otolith calyx fibers (for details, Goldberg et al., 1990b). Third, we would have to know much more about central processing to understand the functional implications of the prevalence of calyx fibers in the cristae. Fourth, there is no need to assume that calyx afferents have only one function related to an extended dynamic range. In fact, regularly-discharging dimorphic and bouton fibers also have low gains and extended dynamic ranges. What distinguishes calyx fibers is a low gain associated with other features of irregularly-discharging fibers, of which phasic response dynamics may be especially relevant. In mammals, such afferents have the most phasic response dynamics (Baird et al., 1988; Lysakowski et al., 1995; Hullar and Minor, 1999; Haque et al., 2004; Ramachandran and Lisberger, 2006; Sadeghi et al., 2007) and, so, in addition to allowing the cristae to handle high-magnitude rotations, these fibers could help to extend the bandwidth of vestibular reflexes (Minor et al., 1999; Huterer and Cullen, 2002; Eatock and Lysakowski, 2006).

Acknowledgments

We are grateful for the expert technical assistance of Mr. Steven Price. Hair cell counts in the otolith organs were begun in collaboration with the late Dr. César Fernández.

LITERATURE CITED

Ali H, Desai SS, Lysakowski A. Comparative cytoarchitectural organization of vertebrate cristae ampullares. Assoc Res Otolaryngol Abstr. 2004:927.

Altshuler DL, Dudley R, McGuire JA. Resolution of a paradox: hummingbird flight at high elevation does not come without a cost. Proc Natl Acad Sci USA. 2004; 101:17731–6. [PubMed: 15598748]

Angelaki DE, Dickman JD. Spatiotemporal processing of linear acceleration: primary afferent and central vestibular neuron responses. J Neurophysiol. 2000; 84:2113–2132. [PubMed: 11024100]

Armand M, Minor LB. Relationship between time- and frequency-domain analyses of angular head movements in the squirrel monkey. J Comput Neurosci. 2001; 11:217–239. [PubMed: 11796939]

Baird RA, Desmadryl G, Fernández C, Goldberg JM. The vestibular nerve of the chinchilla. II. Relation between afferent response properties and peripheral innervation patterns in the semicircular canals. J Neurophysiol. 1988; 60:182–203. [PubMed: 3404216]

Bao H, Wong WH, Goldberg JM, Eatock RA. Voltage-gated calcium channel currents in type I and type II hair cells isolated from the rat crista. J Neurophysiol. 2003; 90:155–164. [PubMed: 12843307]

Behrend O, Schwark C, Kunihiro T, Strupp M. Cyclic GMP inhibits and shifts the activation curve of the delayed-rectifier (I_{K1}) of type I mammalian vestibular hair cells. Neuroreport. 1997; 8:2687–2690. [PubMed: 9295101]

Boyle R, Carey JP, Highstein SM. Morphological correlates of response dynamics and efferent stimulation in horizontal semicircular canal afferents of the toadfish, *Opsanus tau*. J Neurophysiol. 1991; 66:1504–1521. [PubMed: 1765791]

Brichta AM, Aubert A, Eatock RA, Goldberg JM. Regional analysis of whole cell currents from hair cells of the turtle posterior crista. J Neurophysiol. 2002; 88:3259–3278. [PubMed: 12466445]

Brichta AM, Goldberg JM. Morphological identification of physiologically characterized afferents innervating the turtle posterior crista. J Neurophysiol. 2000; 83:1202–23. [PubMed: 10712450]

Brichta AM, Peterson EH. Functional architecture of vestibular primary afferents from the posterior semicircular canal of a turtle, *Pseudemys (Trachemys) scripta elegans*. J Comp Neurol. 1994; 344:481–507. [PubMed: 7929889]

Bulmer, MG. Principles of Statistics. New York: Dover; 1979.

Chen JWY, Eatock RA. Major potassium conductance in type I hair cells from rat semicircular canals: characterization and modulation by nitric oxide. J Neurophysiol. 2000; 841:139–151. [PubMed: 10899192]

Correia MJ, Lang DG. An electrophysiological comparison of solitary type I and type II vestibular hair cells. Neurosci Lett. 1990; 116:106–111. [PubMed: 2259440]

DeGroot JCMJ, Veldman JE, Huizing EH. An improved fixation method for guinea pig cochlear tissue. Acta Otolaryngol (Stockh). 1987; 104:234–242. [PubMed: 3118631]

Desai SS, Hussain A, Lysakowski A. Comparative morphology of rodent vestibular periphery: II. Cristae ampullares. J Neurophysiol. 2005a; 93:267–280. [PubMed: 15240768]

Desai SS, Zeh C, Lysakowski A. Comparative morphology of rodent vestibular periphery: I. Saccular and utricular maculae. J Neurophysiol. 2005b; 93:251–266. [PubMed: 15240767]

Eatock, RA.; Lysakowski, A. Mammalian vestibular hair cells. In: Eatock, RA.; Fay, RR.; Popper, AN., editors. Vertebrate Hair Cells. Berlin: Springer-Verlag; 2006. p. 348-442.

Engström H. On the double innervation of the sensory epithelia of the inner ear. Acta Otolaryngol (Stockh). 1958; 49:109–118. [PubMed: 13532652]

Engström, H. Fourth Symposium on the Role of the Vestibular Organs in Space Exploration. Washington, DC: NASA SP-187, US Gov't Printing Office; 1970. The first-order vestibular neuron; p. 123-135.

Engström H, Bergstrom B, Ades HW. Macula utriculi and macula sacculi in the squirrel monkey. Acta Otolaryngol Suppl. 1972; 301:75–126. [PubMed: 4633788]

Fernández C, Baird RA, Goldberg JM. The vestibular nerve of the chinchilla. I. Peripheral innervation patterns in the horizontal and superior semicircular canals. J Neurophysiol. 1988; 60:167–181. [PubMed: 3404215]

Fernández C, Goldberg JM. Physiology of peripheral neurons innervating semicircular canals of the squirrel monkey. II. Response to sinusoidal stimulation and dynamics of peripheral vestibular system. J Neurophysiol. 1971; 34:661–675. [PubMed: 5000363]

Fernández C, Goldberg JM. Physiology of peripheral neurons innervating otolith organs of the squirrel monkey. II. Directional selectivity and force-response relations. J Neurophysiol. 1976; 39:985–995. [PubMed: 824413]

Fernández C, Goldberg JM. Physiology of peripheral neurons innervating otolith organs of the squirrel monkey. III. Response dynamics. J Neurophysiol. 1976; 39:996–1008. [PubMed: 824414]

Fernández C, Lysakowski A, Goldberg JM. Hair-cell counts and afferent innervation patterns in the cristae ampullares of the squirrel monkey with a comparison to the chinchilla. J Neurophysiol. 1995; 73:1253–1269. [PubMed: 7608769]

Furukawa T, Ishii Y, Matsuura S. Synaptic delay and time course of postsynaptic potentials at the junction between hair cells and eighth nerve fibers in the goldfish. Jpn J Physiol. 1972; 22:617–635. [PubMed: 4347488]

Glowatzki E, Fuchs PA. Transmitter release at the hair cell ribbon synapse. Nat Neurosci. 2002; 5:147–154. [PubMed: 11802170]

Goldberg JM. Theoretical analysis of intercellular communication between the vestibular type I hair cell and its calyx ending. J Neurophysiol. 1996; 76:1942–1957. [PubMed: 8890305]

Goldberg JM, Brichta AM. Evolutionary trends in the organization of the vertebrate crista ampullaris. Otolaryngology - Head & Neck Surgery. 1998; 119:165–171. [PubMed: 9743072]

Goldberg JM, Brichta AM. Functional analysis of whole cell currents from hair cells of the turtle posterior crista. J Neurophysiol. 2002; 88:3279–92. [PubMed: 12466446]

Goldberg JM, Desmadryl G, Baird RA, Fernández C. The vestibular nerve of the chinchilla. IV. Discharge properties of utricular afferents. J Neurophysiol. 1990a; 63:781–790. [PubMed: 2341876]

Goldberg JM, Desmadryl G, Baird RA, Fernández C. The vestibular nerve of the chinchilla. V. Relation between afferent discharge properties and peripheral innervation patterns in the utricular macula. J Neurophysiol. 1990b; 63:791–804. [PubMed: 2341877]

Goldberg JM, Fernández C. Physiology of peripheral neurons innervating semicircular canals of the squirrel monkey. I. Resting discharge and response to constant angular accelerations. J Neurophysiol. 1971a; 34:635–660. [PubMed: 5000362]

Goldberg JM, Fernández C. Physiology of peripheral neurons innervating semicircular canals of the squirrel monkey. III. Variations among units in their discharge properties. J Neurophysiol. 1971b; 34:676–684. [PubMed: 5000364]

Goldberg JM, Lysakowski A, Fernández C. Morphophysiological and ultrastructural studies in the mammalian cristae ampullares. Hear Res. 1990c; 49:89–102. [PubMed: 2292511]

Gulley RL, Bagger-Sjoback D. Freeze-fracture studies on the synapse between the type I hair cell and the calyceal terminal in the guinea-pig vestibular system. J Neurocytol. 1979; 8:591–603. [PubMed: 317909]

Gundersen HJ. Stereology of arbitrary particles. A review of unbiased number and size estimators and the presentation of some new ones, in memory of William R. Thompson. J Microsc. 1986; 143(Pt 1):3–45. [PubMed: 3761363]

Haque A, Angelaki DE, Dickman JD. Spatial tuning and dynamics of vestibular semicircular canal afferents in rhesus monkeys. Exp Brain Res. 2004; 155:81–90. [PubMed: 15064888]

Haque A, Huss D, Dickman JD. Afferent innervation patterns of the pigeon horizontal crista ampullaris. J Neurophysiol. 2006; 96:3293–304. [PubMed: 16943311]

Holt JC, Chatlani S, Lysakowski A, Goldberg JM. Quantal and non-quantal transmission in calyx-bearing fibers of the turtle posterior crista. J Neurophysiol. 2007; 98:1083–1101. [PubMed: 17596419]

Holt JC, Xue J-T, Brichta AM, Goldberg JM. Transmission between type II hair cells and bouton afferents in the turtle posterior crista. J Neurophysiol. 2006; 95:428–452. [PubMed: 16177177]

Honrubia V, Hoffman LF, Sitko S, Schwartz IR. Anatomic and physiological correlates in bullfrog vestibular nerve. J Neurophysiol. 1989; 61:688–701. [PubMed: 2786056]

Hullar TE, Della Santina CC, Hirvonen T, Lasker DM, Carey JP, Minor LB. Responses of irregularly discharging chinchilla semicircular canal vestibular-nerve afferents during high-frequency head rotations. J Neurophysiol. 2005; 93:2777–2786. [PubMed: 15601735]

Hullar TE, Minor LB. High-frequency dynamics of regularly discharging canal afferents provide a linear signal for angular vestibuloocular reflexes. J Neurophysiol. 1999; 82:2000–2005. [PubMed: 10515990]

Hurley KM, Gaboyard S, Zhong M, Price SD, Wooltorton JR, Lysakowski A, Eatock RA. M-like K^+ currents in type I hair cells and calyx afferent endings of the developing rat utricle. J Neurosci. 2006; 26:10253–10269. [PubMed: 17021181]

Huterer M, Cullen KE. Vestibuloocular reflex dynamics during high-frequency and high-acceleration rotations of the head on body in rhesus monkey. J Neurophysiol. 2002; 88:13–28. [PubMed: 12091529]

Igarashi M, Watanuki K, Miyata H, Alford BR. Vestibular end organ mapping in the squirrel monkey. Arch Otorhinolaryngol. 1975; 211:153–161. [PubMed: 55117]

Igic PG, Brichta AM. A comparison of horizontal and posterior crista afferent discharge properties in the turtle. Assoc Res Otolaryngol Abs. 1997:139.

Jørgensen JM. The sensory epithelia of the inner ear of two turtles, *Testudo graeca* L. and *Pseudemys scripta* (Schoepff). Acta Zool (Stockh). 1974; 55:289–298.

Jørgensen JM, Andersen T. On the structure of the avian maculae. Acta Zool (Stockh). 1973; 54:121–130.

Keen EC, Hudspeth AJ. Transfer characteristics of the hair cell's afferent synapse. Proc Natl Acad Sci USA. 2006; 103:5537–42. [PubMed: 16567618]

Leonard RB, Kevetter GA. Molecular probes of the vestibular nerve. I. Peripheral termination patterns of calretinin, calbindin and peripherin containing fibers. Brain Res. 2002; 928:8–17. [PubMed: 11844467]

Li A, Xue J, Peterson EH. Architecture of the mouse utricle: macular organization and hair bundle heights. J Neurophysiol. 2008; 99:718–33. [PubMed: 18046005]

Lim, DJ. The development and structure of the otoconia. In: Friedmann, I.; Ballantyne, J., editors. Ultrastructural Atlas of the Inner Ear. London: Butterworths; 1984. p. 245-269.

Lindeman HH. Studies on the morphology of the sensory regions of the vestibular apparatus. Ergeb Anat Entwicklungsgesch. 1969; 42:1–113. [PubMed: 5310109]

Lopez I, Ishiyama G, Tang Y, Tokita J, Baloh RW, Ishiyama A. Regional estimates of hair cells and supporting cells in the human crista ampullaris. J Neurosci Res. 2005; 82:421–431. [PubMed: 16211560]

Lysakowski A. Synaptic organization of the crista ampullaris in vertebrates. Ann NY Acad Sci. 1996; 781:164–182. [PubMed: 8694413]

Lysakowski A, Goldberg JM. A regional ultrastructural analysis of the cellular and synaptic architecture in the chinchilla cristae ampullares. J Comp Neurol. 1997; 389:419–443. [PubMed: 9414004]

Lysakowski, A.; Goldberg, JM. Morphophysiology of the vestibular periphery. In: Highstein, SM.; Popper, A.; Fay, RR., editors. The Vestibular System. New York: Springer-Verlag; 2004. p. 57-152.

Lysakowski A, Minor LB, Fernández C, Goldberg JM. Physiological identification of morphologically distinct afferent classes innervating the cristae ampullares of the squirrel monkey. J Neurophysiol. 1995; 73:1270–1281. [PubMed: 7608770]

MacDougall HG, Moore ST. Marching to the beat of the same drummer: the spontaneous tempo of human locomotion. J Appl Physiol. 2005; 99:1164–1173. [PubMed: 15890757]

Malenka RC, Bear MF. LTP and LTD: an embarrassment of riches. Neuron. 2004; 44:5–21. [PubMed: 15450156]

Matsubara A, Takumi Y, Nakagawa T, Usami S, Shinkawa H, Ottersen OP. Immunoelectron microscopy of AMPA receptor subunits reveals three types of putative glutamatergic synapse in the rat vestibular end organs. Brain Res. 1999; 819:58–64. [PubMed: 10082861]

Merchant SN, Velazquez-Villasenor L, Tsuji K, Glynn RJ, Wall C 3rd, Rauch SD. Temporal bone studies of the human peripheral vestibular system. Normative vestibular hair cell data. Ann Otol Rhinol Laryngol Suppl. 2000; 181:3–13. [PubMed: 10821229]

Minor LB, Lasker DM, Backous DD, Hullar TE. Horizontal vestibuloocular reflex evoked by high-acceleration rotations in the squirrel monkey. I. Normal responses. J Neurophysiol. 1999; 82:1254–1270. [PubMed: 10482745]

Myers SE, Lewis ER. Hair cell tufts and afferent innervation of the bullfrog crista ampullaris. Brain Res. 1990; 534:15–24. [PubMed: 1705850]

Nowak, RM.; Paradiso, JL. Walker's mammals of the world. Vol. 1. Baltimore: Johns Hopkins Univ Press; 1983.

Plotnik M, Goldberg JM, Marlinski VV. Excitatory response-intensity relations in afferent from the chinchilla's superior and horizontal canals. Soc Neurosci Abstr. 1999; 25:663.

Pozzo T, Berthoz A, Lefort L. Head stabilization during various locomotor tasks in humans. I. Normal subjects. Exp Brain Res. 1990; 82:97–106. [PubMed: 2257917]

Ramachandran R, Lisberger SG. Transformation of vestibular signals into motor commands in the vestibulo-ocular reflex pathways of monkeys. J Neurophysiol. 2006; 96:1061–1074. [PubMed: 16760348]

Rennie K, Correia MJ. Potassium currents in mammalian and avain isolated type I semicircular canal hair cells. J Neurophysiol. 1994; 71:317–329. [PubMed: 8158233]

Rennie KJ, Streeter MA. Voltage-dependent currents in isolated vestibular afferent calyx terminals. J Neurophysiol. 2006; 95:26–32. [PubMed: 16162827]

Richardson KC, Jarett L, Finke EH. Embedding in epoxy resins for ultrathin sectioning in electron microscopy. Stain Technol. 1960; 35:313–323. [PubMed: 13741297]

Rosenhall U. Vestibular macular mapping in man. Ann Otol Rhinol Laryngol. 1972; 81:339–351. [PubMed: 4113136]

Rossi ML, Martini M, Pelucchi B, Fesce R. Quantal nature of synaptic transmission at the cytoneural junction in the frog labyrinth. J Physiol (Lond). 1994; 478:17–35. [PubMed: 7965832]

Rüsch A, Eatock RA. A delayed rectifier conductance in type I hair cells of the mouse utricle. J Neurophysiol. 1996; 76:995–1004. [PubMed: 8871214]

Sadeghi SG, Minor LB, Cullen KE. Response of vestibular-nerve afferents to active and passive rotations under normal conditions and after unilateral labyrinthectomy. J Neurophysiol. 2007; 97:1503–1514. [PubMed: 17122313]

Schessel DA, Ginzberg R, Highstein SM. Morphophysiology of synaptic transmission between type I hair cells and vestibular primary afferents. An intracellular study employing horseradish peroxidase in the lizard, *Calotes versicolor*. Brain Res. 1991; 544:1–16. [PubMed: 1713111]

Si X, Zakir MM, Dickman JD. Afferent innervation of the utricular macula in pigeons. J Neurophysiol. 2003; 89:1660–1677. [PubMed: 12626631]

Smith, CA.; Rasmussen, GL. Third Symposium on the Role of the Vestibular Organs in Space Exploration. Washington, DC: NASA SP-152, US Gov't Printing Office; 1967. Nerve endings in the maculae and cristae of the chinchilla vestibule, with a special reference to the efferents; p. 183-201.

Smith CE, Goldberg JM. A stochastic afterhyperpolarization model of repetitive activity in vestibular afferents. Biol Cybern. 1986; 54:41–51. [PubMed: 3487348]

Spoendlin, H. Second Symposium on the Role of the Vestibular Organs in Space Exploration. Washington, DC: NASA SP-115, US Gov't Printing Office; 1966. Some morphofunctional and pathological aspects of the vestibular sensory epithelia; p. 99-116.

Tobalske BW, Warrick DR, Clark CJ, Powers DR, Hedrick TL, Hyder GA, Biewener AA. Three-dimensional kinematics of hummingbird flight. J Exp Biol. 2007; 210:2368–2382. [PubMed: 17575042]

Watanuki K, Meyer zum Gottesberge A. Light microscopic observations of the sensory epithelium of the crista ampullaris in the guinea pig. Ann Otol Rhinol Laryngol. 1971; 80:450–454. [PubMed: 4102921]

Weimerskirch H, Chastel O, Barbraud C, Tostain O. Flight performance: Frigatebirds ride high on thermals. Nature. 2003; 421:333–334. [PubMed: 12540890]

Wersäll, J.; Bagger-Sjöbäck, D. Morphology of the vestibular sense organ. In: Kornhuber, HH., editor. Handbook of Sensory Physiology, Vestibular System Basic Mechanisms. Berlin: Springer-Verlag; 1974. p. 123-170.

Xue J, Peterson EH. Hair bundle heights in the utricle: differences between macular locations and hair cell types. J Neurophysiol. 2006; 95:171–186. [PubMed: 16177175]

Zakir M, Huss D, Dickman JD. Afferent innervation patterns of the saccule in pigeons. J Neurophysiol. 2003; 89:534–550. [PubMed: 12522200]

Ziff EB. TARPs and the AMPA receptor trafficking paradox. Neuron. 2007; 53:627–633. [PubMed: 17329203]

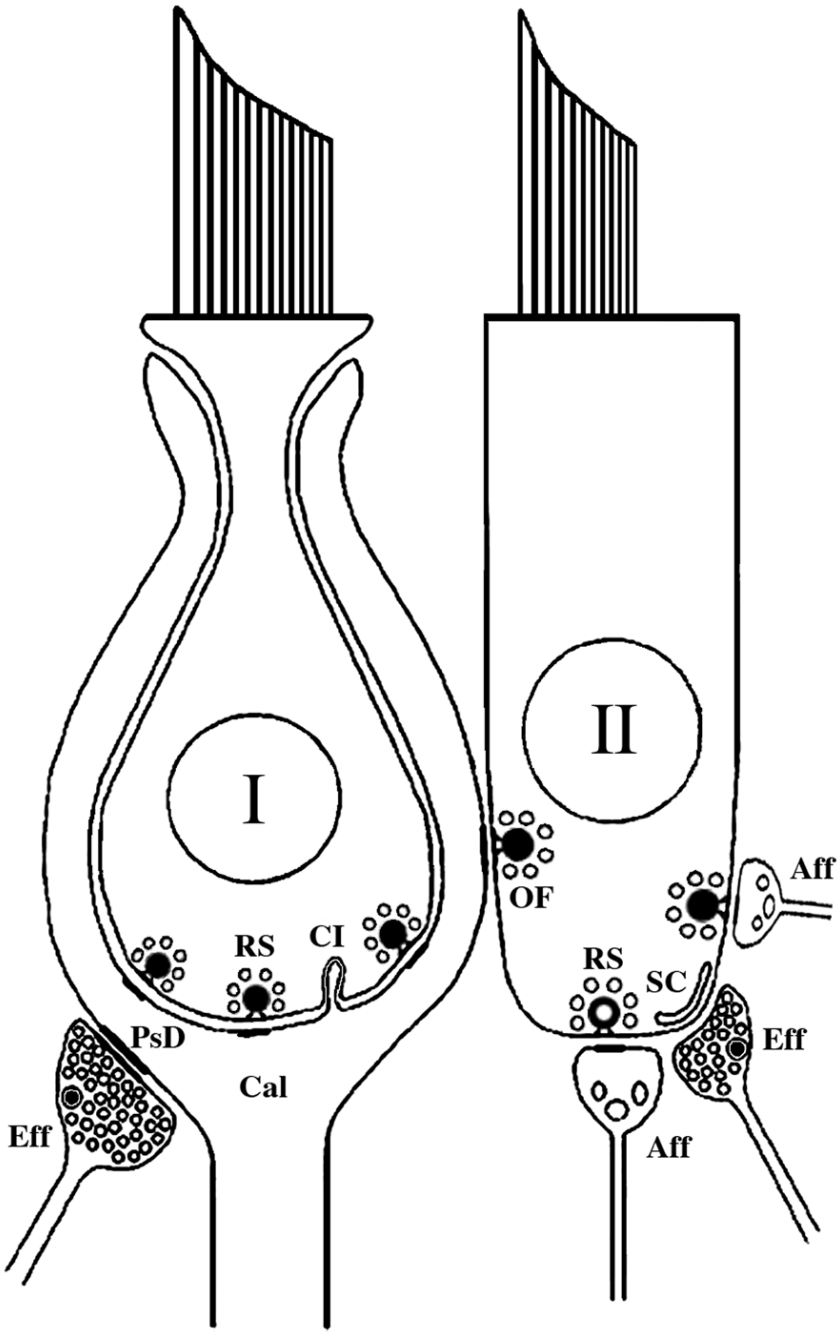

Figure 1.
Synaptic elements on type I and type II hair cells. Calyx endings (*Cal*) surround the basolateral surface of type I (*I*) hair cells and make calyceal invaginations (*CI*) into the hair cell. Afferent boutons (*Aff*) synapse with type II (*II*) hair cells. Ribbon synapses (*RS*) are located in both hair cells. Outer-face ribbon synapses (*OF*) are made by type II hair cells onto calyx endings. Efferent endings (*Eff*) on calyces are marked by a postsynaptic density (*PSD*) while those on type II hair cells are marked by a subsynaptic cistern (*SC*).

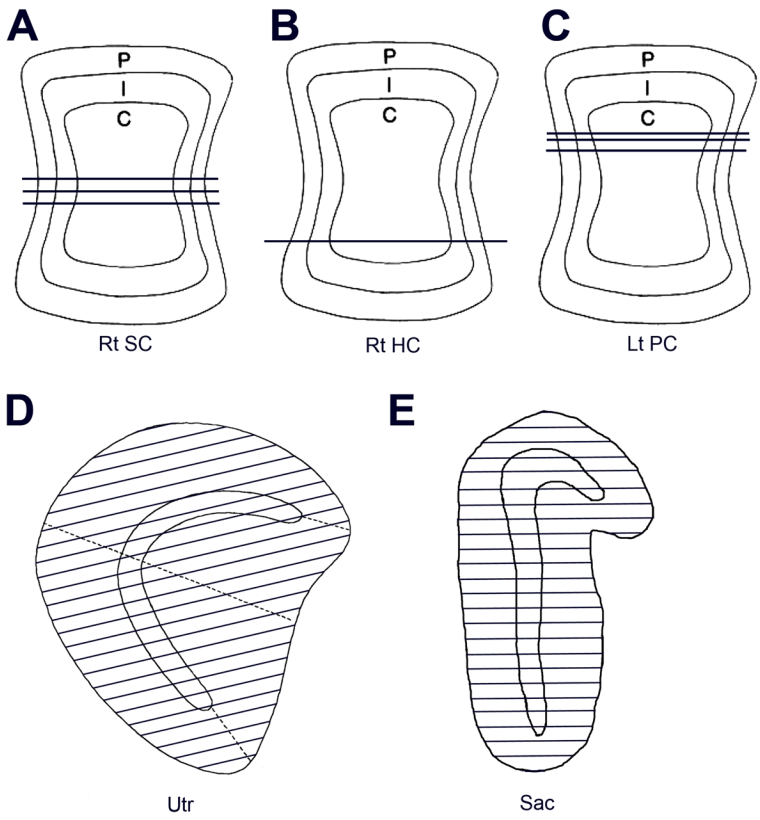

Figure 2.

Samples based on surface reconstructions are shown after transfer to standard drawings. **A–C.** Thirty-section transverse ultrathin samples in three cristae, each taken from a different animal. Seven samples were analyzed, three in each of two animals (*A, C*) and one in a third animal (*B*). *Rt SC, Rt HC* and *Lt PC*, right superior, right horizontal and left posterior cristae. **D, E.** Hair cells were counted in 2-μm transverse sections throughout the utricular (*D, Utr*) and saccular (*E, Sac*) maculae. Lines in each drawing spaced 50 μm apart show the sections in a single organ. Samples, each taken from a different labyrinth, were similar in three other utricular and one other saccular organs.

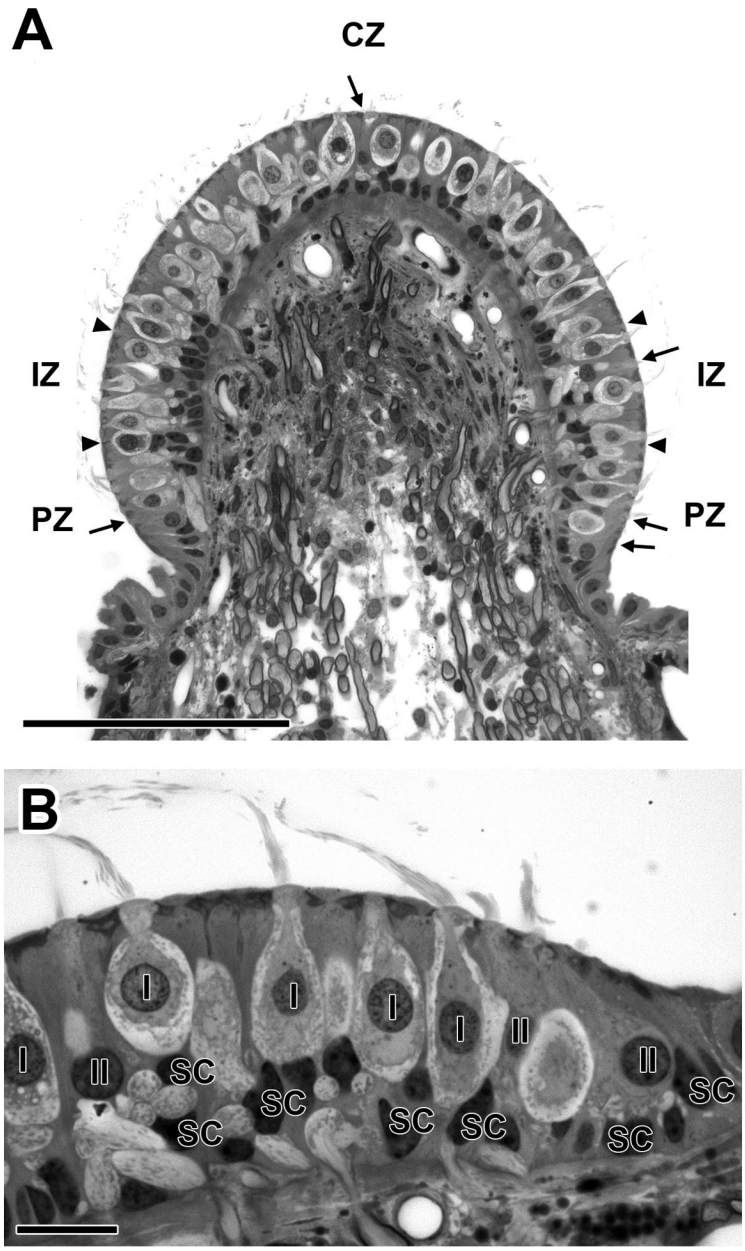

Figure 3.

Morphology of the squirrel monkey crista. **A.** Cross-section of a superior crista. There is a preponderance of type I hair cells. The few type II hair cells are marked by arrows. Boundaries between central (*CZ*), intermediate (*IZ*) and peripheral (*PZ*) zones are indicated by arrowheads. **B.** The intermediate and peripheral zones on the right in ***A*** are seen at higher magnification. Five type I hair cells (*I*) with nuclei are surrounded by calyces. Three type II hair cells (*II*) are seen. Supporting-cell nuclei (*SC*) are at the bottom. Scale bars, 100 μm (*A*) and 10 μm (*B*).

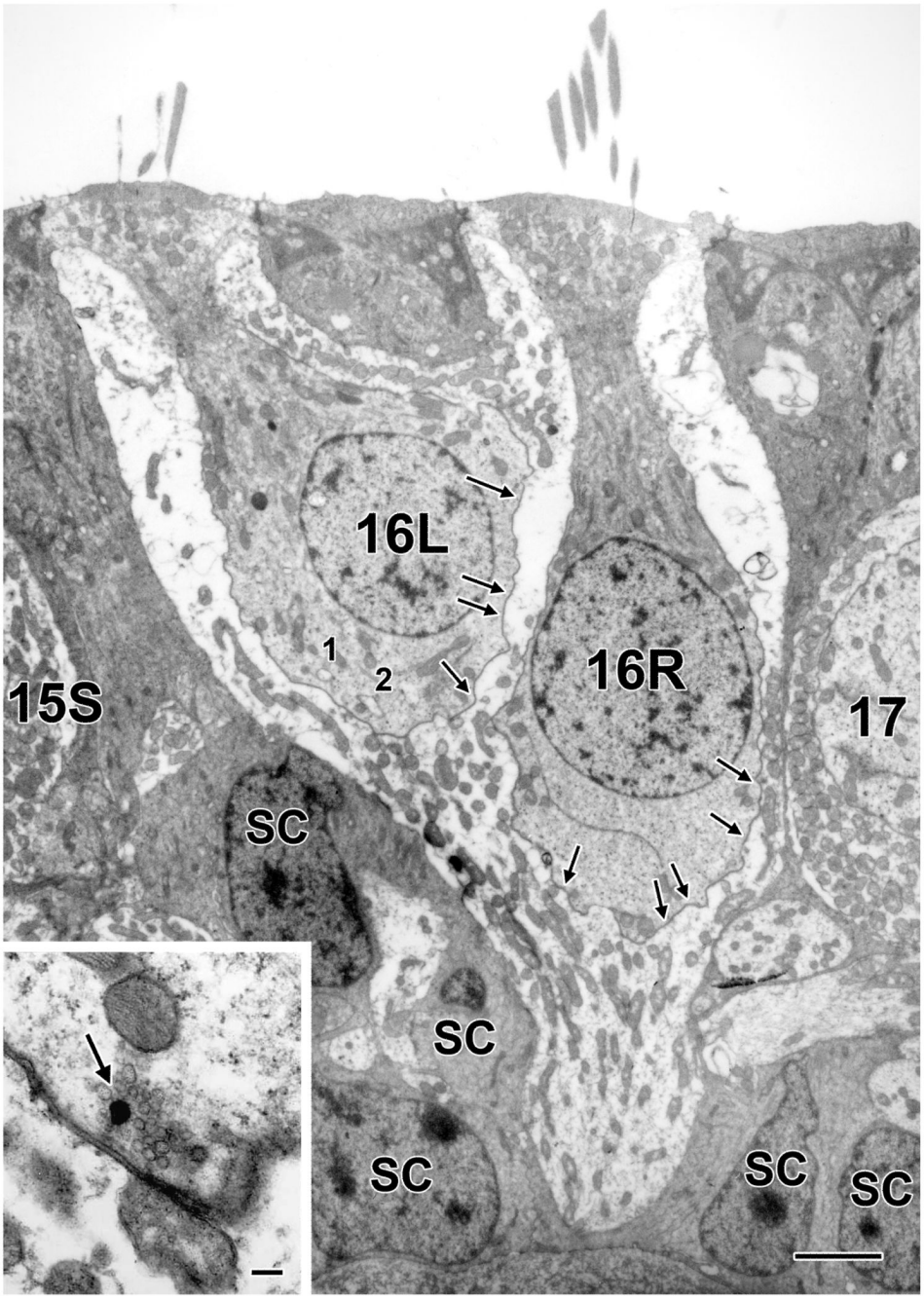

Figure 4.
Central type I hair cells. Two such hair cells (*16L, 16R*) from a superior crista are enclosed in a complex calyx sandwiched between supporting cells (*SC*). The locations of ribbon synapses present in this section and in neighboring sections in this figure and in Figures 5 and 6 are indicated by arrows. One ribbon is shown at higher magnification in the inset *(arrow)*. Two invaginations (*1* and *2*) in the hair cell on the left can be traced to the synaptic cleft in another section. In this and other figure legends, the numbers of synaptic features are for the disector sample of 30 ultrathin sections. Scale bars, 2 μm (*main figure*) and 0.2 μm (*inset*).

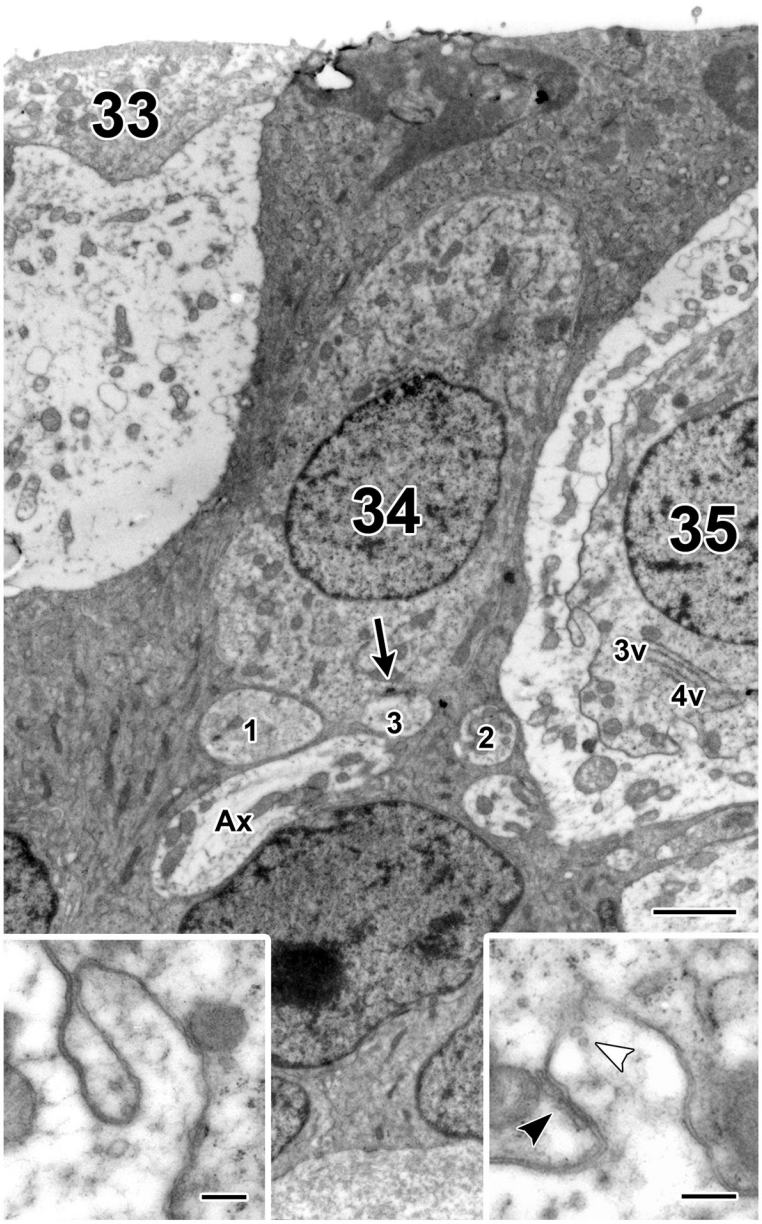

Figure 5.

Central type II hair cell. A central type II hair cell (*34*) is flanked by the calyx endings of two type I hair cells (*33* and *35*) and a large axonal process (*Ax*) passes nearby. Of the four afferent boutons contacting cell 34, only three of them (*1,2,3*) are seen here and only bouton 3 has a synapse in the sample (arrow). Bouton 2 has moved away from cell 34 in this section. As for the type I hair cells, cell 35 had two ribbons and 15 invaginations; two of the invaginations (*3v* and *4v*) are present in the section (see *insets, arrowheads*). White arrowhead in right *inset* indicates small vesicles sometimes present near the upper end of an invagination. Black arrowhead in right *inset* shows smooth endoplasmic reticulum adjacent to the invagination (see also Fig. 7). Only a small remnant of cell 33 is present above its calyx ending and no afferent synapses were observed in this cell. Neither calyx ending was contacted by efferent boutons. Scale bars, 2 μm (*main figure*) and 0.5 μm (*insets*).

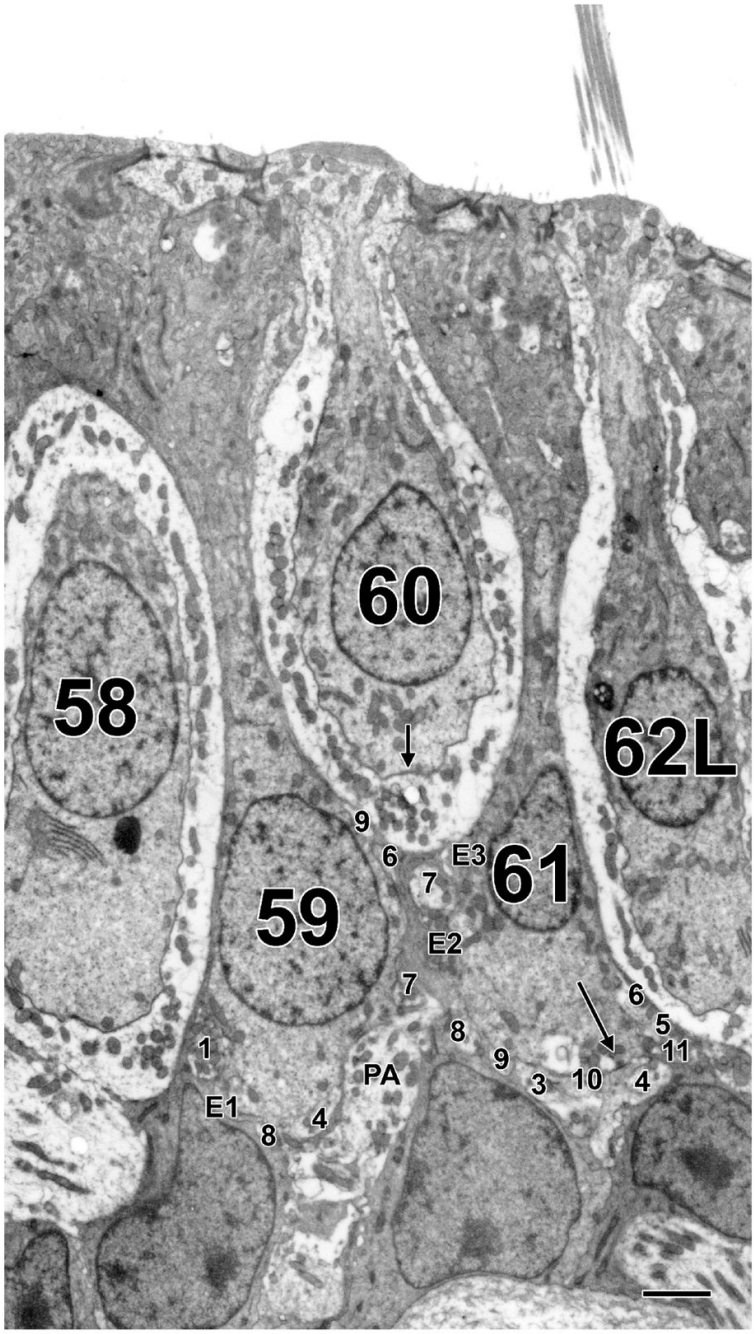

Figure 6.

Peripheral zone, type I and type II hair cells. Two type II hair cells (*59* and *61*) are intercalated between three type I hair cells (*58, 60* and *62L*). The large process to the right of cell 59 is the parent axon (*PA*) of the calyx innervating cell 60. Several afferent boutons, designated by numbers, are seen on each type II hair cell. Efferent boutons are designated by the letter *E*. Both afferent and efferent boutons are numbered as they appeared from the start of the sample. Long arrow in cell 61 indicates ribbon present in this section. Scale bar, 2 μm.

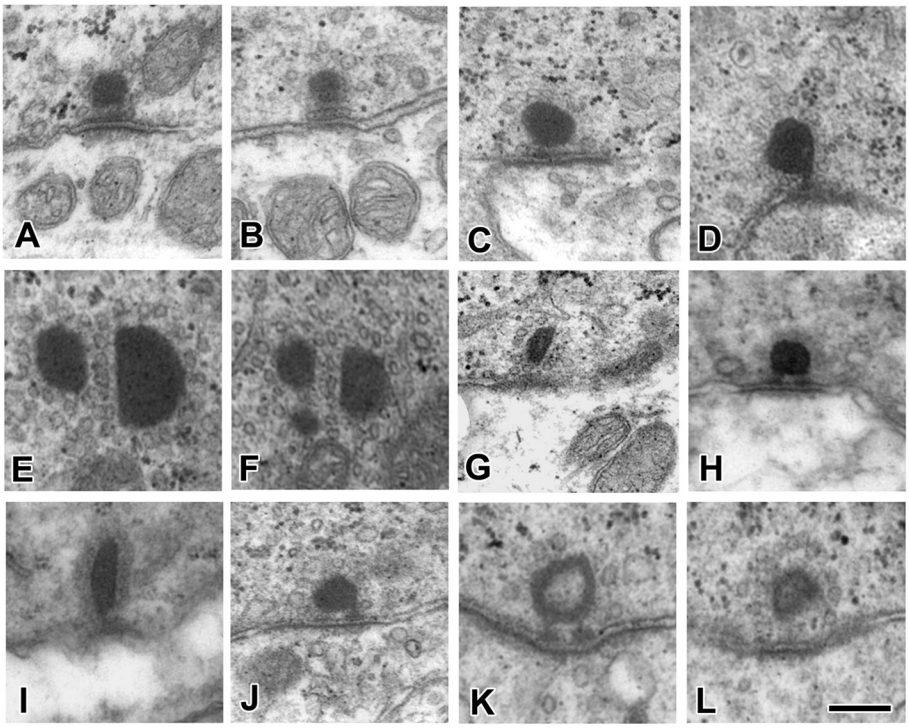

Figure 7.

Examples of ribbon synapses from type I hair cells in the central (**A**) and peripheral zones (**B**) and from type II hair cells in the central (**C**–**G**), intermediate (**H, I**) and peripheral zones (**J**–**L**). Synapses in *C, D* and *I–L* contact afferent boutons; *E–H* are outer-face ribbons. *E* and *F* are near-adjacent sections through three ribbons forming an outer-face cluster. Docked vesicles are especially prominent in *B*. Pedicles connecting the synaptic body with the plasmalemma are seen in *C, D, H, J* and *K.* Scale bar, 0.2 μm.

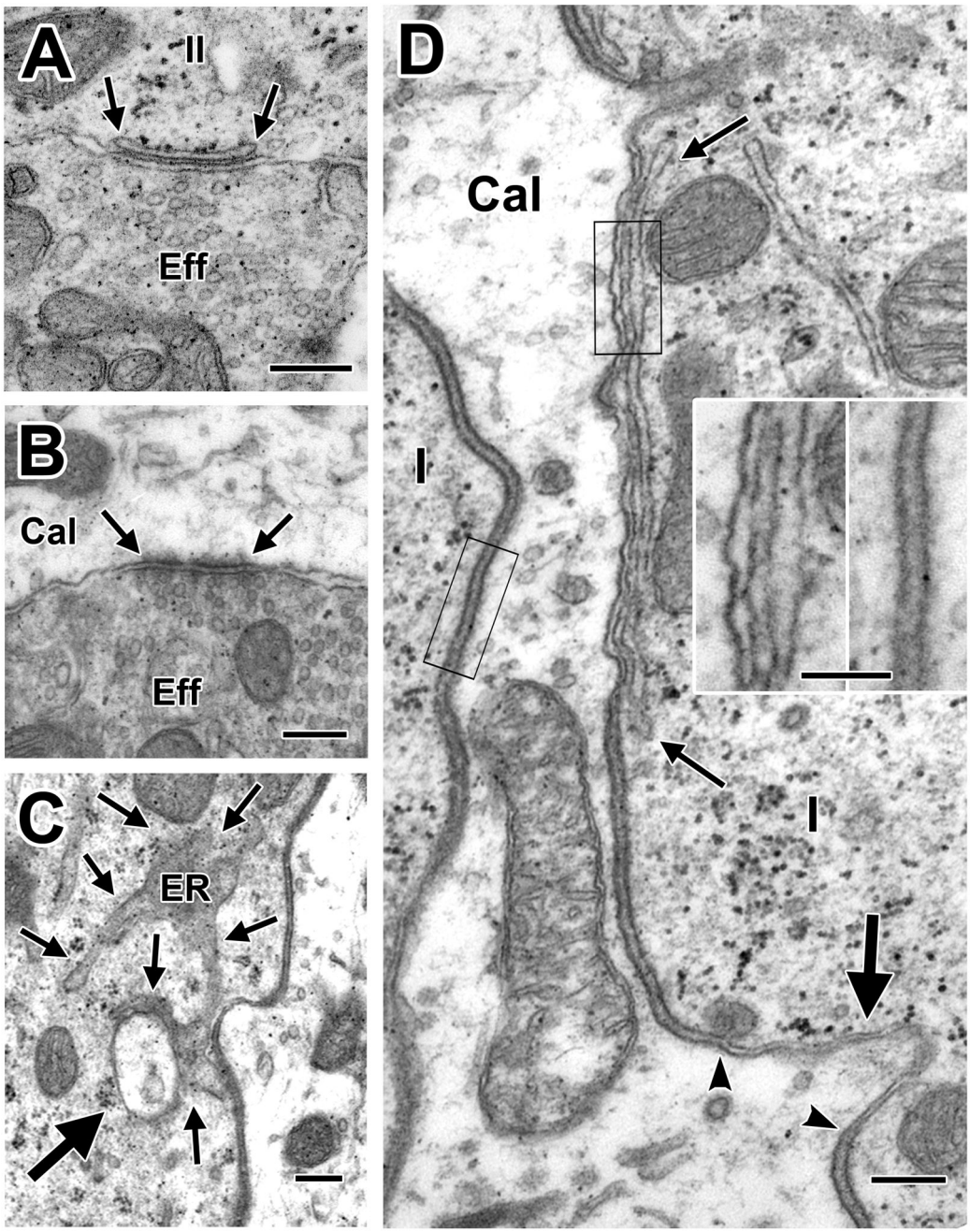

Figure 8.

Efferent innervation, invaginations and subsurface cisterns. **A, B.** Highly vesiculated efferent boutons contact a type II hair cell and a calyx ending, respectively. **C.** A calyx ending invaginates into a type I hair cell. The invagination, including a pinched off portion (thick arrow), is in close association with the endoplasmic reticulum (*ER, thin arrows*). **D.** At the location of a subsurface cistern (delimited by *thin arrows*) in a type I hair cell (I) adjacent to the inside wall of a complex calyx (*Cal*), there is a narrowing of the intercellular space, similar to that seen at a neighboring invagination (*thick arrow,* the narrow extracellular cleft of the invagination is delimited by *arrowheads*). The calyx membrane narrows roughly 60% near the cistern from about 8.5 nm, on average, to 5.2 nm, as seen in

the *insets* taken from the areas indicated by the two black rectangles in *D*. Scale bars, 0.2 μm (*A*–*D*) and 0.1 μm (*insets*).

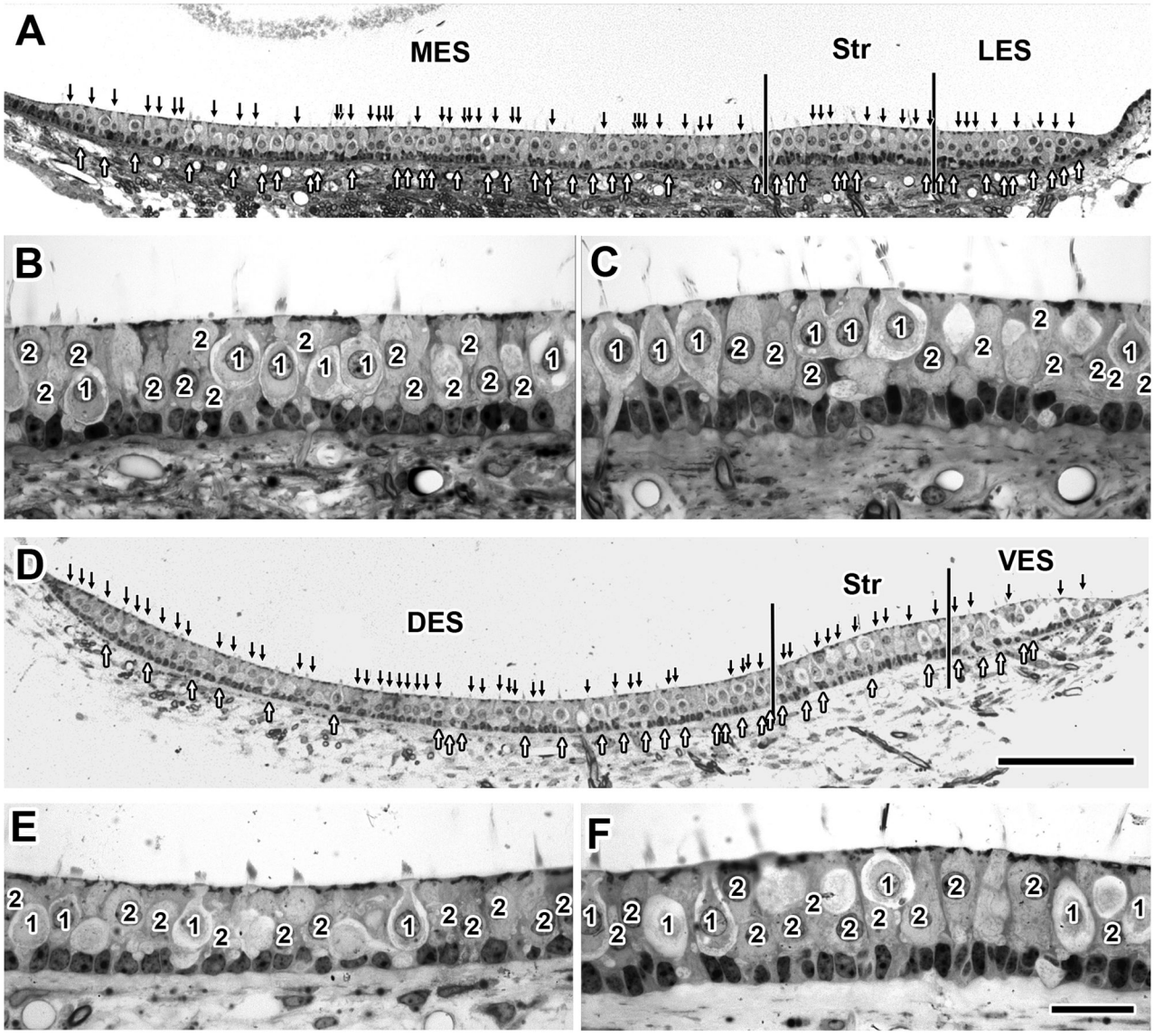

Figure 9.

Type I and type II hair cells, utricular and saccular maculae. **A, D.** Low-power micrographs of the utricular and saccular maculae, respectively. Arrows above *(black)* and underneath *(white)* each neuroepithelium mark type II and type I hair cells, respectively. Vertical lines border the striolar region *(Str)* in each case. Medial (*MES*) and lateral (*LES*) extrastriola are marked in the utricular macula (*A*), and dorsal *(DES)* and ventral *(VES)* extrastriola are indicated in the saccular macula (*D*). **B, C.** High-power micrographs from, respectively, the MES and Str regions of the utricular macula. **E, F.** High-power micrographs from, respectively, the DES and Str regions of the saccular macula. Scale bars, 100 μm (*D*) also holds for *A;* 20 μm *(F*) also holds for *B, C* and *E.*

Table 1

Number of hair cells, various zones of crista, squirrel monkey and chinchilla

Zone	Type I	Type II	Type I : Type II ratio
Central			
Squirrel monkey--EM	41	13	3.2 ± 0.7
Squirrel monkey --LM	448	86	5.2 ± 0.5
Chinchilla--EM	50	58	0.9 ± 0.1
Chinchilla--LM	284	252	1.1 ± 0.9
Intermediate			
Squirrel monkey--EM	27	9	3.0 ± 0.8
Squirrel monkey --LM	630	147	4.2 ± 0.8
Chinchilla--EM	40	30	1.3 ± 0.1
Chinchilla--LM	480	376	1.3 ± 0.1
Peripheral			
Squirrel monkey--EM	14	7	2.0 ± 0.4
Squirrel monkey --LM	445	301	1.5 ± 0.1
Chinchilla--EM	23	30	0.8 ± 0.03
Chinchilla--LM	456	528	0.9 ± 0.03
All			
Squirrel monkey--EM	82	29	2.8 ± 1.0
Squirrel monkey --LM	1,523	534	2.8 ± 0.2
Chinchilla--EM	113	118	1.0 ± 0.07
Chinchilla--LM	1,220	1,156	1.1 ± 0.03

EM, electron microscopy; LM, light microscopy; Type I and Type II, total number of hair cells counted. Type I : Type II ratio ± SE. Squirrel monkey—EM (this study); Squirrel monkey—LM and Chinchilla—LM (Fernández et al., 1995); Chinchilla—EM (Lysakowski and Goldberg, 1997). Number of samples: Squirrel monkey—EM (7); Squirrel monkey—LM (8); Chinchilla—EM (10); Chinchilla—LM (8).

Table 2

Synaptic features per type I hair cell, various zones of crista

Zone	Inner-face ribbons	Calyceal invaginations	Efferent boutons	Outer-face ribbons
Central	9.3 ± 1.2 (22 ± 4)	20.3 ± 2.4 ** (53 ± 8)	1.6 ± 0.3 (2.9 ± 0.5)	0.22 ± 0.10 (2.9 ± 0.6)
Intermediate	6.5 ± 1.1 (17 ± 2)	13.2 ± 3.9 (17 ± 2)	1.1 ± 0.3 (3.2 ± 0.5)	0.22 ± 0.10 (1.0 ± 0.4)
Peripheral	8.9 ± 1.4 (10 ± 1)	3.7 ± 0.9 ** (10 ± 2)	0.7 ± 0.3 (3.3 ± 0.4)	0 (0.1 ± 0.1)
All	8.3 ± 0.9 (17 ± 2)	15.1 ± 2.2 (28 ± 5)	1.4 ± 0.3 (3.1 ± 0.3)	0.18 ± 0.05 (1.4 ± 0.3)

** Upper values, squirrel monkey; lower values (in parentheses), chinchilla from Lysakowski and Goldberg (1997). Number of samples: squirrel monkey (7); chinchilla (10). Differences between central and peripheral zones, squirrel monkey, $p < 0.01$.

Table 3

Synaptic features per type II hair cell, various zones of crista

Zone	Ribbons on boutons	Afferent boutons	Efferent boutons	Ribbons on calyx endings
Central	12.9 ± 2.1 ** (15 ± 1)	11.8 ± 2.0 * (9 ± 1)	3.0 ± 1.3 (3.5 ± 0.4)	0.7 ± 0.3 (2.5 ± 0.5)
Intermediate	12.9 ± 3.6 (22 ± 2)	17.0 ± 3.9 (22 ± 3)	1.6 ± 0.6 (2.5 ± 0.4)	0.7 ± 0.3 (1.0 ± 0.1)
Peripheral	39.0 ± 9.8 ** (17 ± 2)	32.1 ± 8.8 * (22 ± 2)	6.0 ± 2.3 (2.5 ± 0.4)	0 (0.8 ± 0.2)
All	19.3 ± 2.7 (18 ± 1)	18.4 ± 2.9 (22 ± 2)	3.6 ± 1.1 (3.5 ± 0.3)	0.5 ± 0.2 (1.2 ± 0.2)

Upper values, squirrel monkey; lower values (in parentheses), chinchilla from Lysakowski and Goldberg (1996). Number of samples: squirrel monkey (7); chinchilla (10). Differences between central and peripheral zones, squirrel monkey,

* $p < 0.02$ and

** $p < 0.01$.

Table 4

Appositions and outer-face synapses, various zones of crista, squirrel monkey

Zone	Type I hair cells	Appositions	Outer-face synapses
Central	160	25/160 (16%)	6/25 (24%)
Intermediate	102	27/102 (26%)	6/27 (22%)
Peripheral	41	16/41 (39%)	0/16 (0%)
All	303	68/303 (22%)	12/68 (18%)

Second column, all type I hair cells with nuclei, six samples. Third column, ratio of appositions to hair cells. Fourth column, ratio of outer face synapses to appositions.

Table 5

Number of hair cells and ratio of type I to type II hair cells, otolith organs of squirrel monkey.

			Striola		Anterolateral/ventral extrastriola		Medial/dorsal extrastriola		All zones	
	N	**Total No. HCs**	**%HC**	**I : II ratio**	**%HC**	**I : II ratio**	**%HC**	**I : II ratio**	**%HC**	**I : II ratio**
Utriculus	4	18,200 ± 1000	7	0.59 ± 0.03	48	0.54 ± 0.05	45	0.65 ± 0.05	100	0.59 ± 0.06
				0.63 ± 0.11		0.53 ± 0.06		0.63 ± 0.11		
Sacculus	2	12,100 ± 720	12	0.59 ± 0.13	29	0.55 ± 0.09	59	0.51 ± 0.11	100	0.53 ± 0.06

N, number of organs counted. *Total No. HCs,* total number of hair cells in organ. *%HC,* percentage of hair cells in zone to total number. *I : II ratio,* ratio of type I to type II hair cells; entries are mean ratio ± SEM. Anterolateral (utriculus) and ventral (sacculus) extrastriola. Medial (utriculus) and dorsal (sacculus) extrastriola. Two ratios are given for the utriculus, one with the line of polarity reversal (LPR) taken as the center line of the striola *(upper)* and the other with the LPR as the lateral border of the striola *(lower)*.